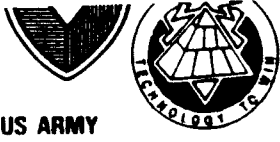


AD-A256 077



AD

2



US ARMY  
LABORATORY COMMAND  
MATERIALS TECHNOLOGY LABORATORY

MTL TR 92-36

# HAFNIUM- AND TITANIUM-COATED TUNGSTEN POWDERS FOR KINETIC ENERGY PENETRATORS, PHASE I, SBIR

May 1992

BRIAN E. WILLIAMS and JACOB J. STIGLICH, Jr.  
Ultramet  
12173 Montague Street  
Pacoima, CA 91331

DTIC  
ELECTE  
OCT 05 1992

FINAL REPORT

Contract DAAL04-91-C-0022

Approved for public release; distribution unlimited.

92 1 1 12

92-26377



77PX

Prepared for

U.S. ARMY MATERIALS TECHNOLOGY LABORATORY  
Watertown, Massachusetts 02172-0001

The findings in this report are not to be construed as an official Department of the Army position, unless so designated by other authorized documents.

Mention of any trade names or manufacturers in this report shall not be construed as advertising nor as an official indorsement or approval of such products or companies by the United States Government.

**DISPOSITION INSTRUCTIONS**

**Destroy this report when it is no longer needed.  
Do not return it to the originator**

4. PERFORMING ORGANIZATION REPORT NUMBER(S) ULT/TR-91-7670			5. MONITORING ORGANIZATION REPORT NUMBER(S)		
6a. NAME OF PERFORMING ORGANIZATION Ultramet		6b. OFFICE SYMBOL (if applicable)	7a. NAME OF MONITORING ORGANIZATION		
6c. ADDRESS (City, State, and ZIP Code) 12173 Montague Street Pacoima, CA 91331			7b. ADDRESS (City, State, and ZIP Code)		
8a. NAME OF FUNDING/SPONSORING ORGANIZATION U.S. Army		8b. OFFICE SYMBOL (if applicable) SLCMT-PR	9. PROCUREMENT INSTRUMENT IDENTIFICATION NUMBER DAAL04-91-C-0022 MTL TR 92-36		
8c. ADDRESS (City, State, and ZIP Code) Materials Technology Laboratory Watertown, MA 02172-0001			10. SOURCE OF FUNDING NUMBERS		
	PROGRAM ELEMENT NO.	PROJECT NO.	TASK NO	WORK UNIT ACCESSION NO.	
11. TITLE (Include Security Classification) HAFNIUM- TITANIUM-COATED TUNGSTEN POWDERS FOR KINETIC ENERGY PENETRATORS, PHASE I, SBIR					
12. PERSONAL AUTHOR(S) Brian E. Williams and Jacob J. Stiglich, Jr.					
13a. TYPE OF REPORT Final Technical		13b. TIME COVERED FROM 2/91 TO 10/91		14. DATE OF REPORT (Year, Month, Day) May 1992	15. PAGE COUNT 71
16. SUPPLEMENTARY NOTATION Small Business Innovation Research (SBIR) Program, Phase I					
17. COSATI CODES			18. SUBJECT TERMS (Continue on reverse if necessary and identify by block number)		
FIELD	GROUP	SUB-GROUP	Tungsten powders, Composites, Chemical vapor deposition (CVD), Microstructure, Hafnium, Titanium, Dynamic tests, Strain rate testing, Powder metallurgy		
11	03				
11	06	(01)			
19. ABSTRACT (Continue on reverse if necessary and identify by block number) Depleted uranium (DU) is the state-of-the-art material for kinetic energy penetrators used to defeat steel and composite armors. DU alloys, however, are costly to fabricate, handle, and store because of their extremely complex metallurgy and the obvious health considerations associated with the use of uranium. Tungsten composite materials are also used in kinetic energy penetrators, offering easier and safer fabrication, handling, and storage but to date lacking the performance of DU. The mechanisms by which a penetrator defeats an armor are difficult to determine, either experimentally or from first principles. Recent experiments have identified the presence of an "adiabatic shear" mechanism that appears to be important in the penetration of rolled homogeneous armor (RHA) by DU penetrators. In this program, Ultramet proposed to apply hafnium and titanium coatings to tungsten powder ( $W_p$ ) particles by chemical vapor deposition (CVD) using an established fluidized-bed powder coating technique. Both hafnium and titanium are known to exhibit the adiabatic shear phenomenon. High strain rate experiments ( $\approx 10^4$ /sec) were performed on Ti(6Al-4V) and (continued)					
20. DISTRIBUTION/AVAILABILITY OF ABSTRACT <input checked="" type="checkbox"/> UNCLASSIFIED/UNLIMITED <input type="checkbox"/> SAME AS RPT. <input type="checkbox"/> DTIC USERS			21. ABSTRACT SECURITY CLASSIFICATION Unclassified		
22a. NAME OF RESPONSIBLE INDIVIDUAL Robert J. Dowding			22b. TELEPHONE (Include Area Code) 617-923-5340	22c. OFFICE SYMBOL SLCMT-MEN	

Block 19 continued:

monolithic hafnium materials in order to establish the presence or absence of this mode of deformation in small cylindrical specimens. In addition, specimens of 2 wt% CVD Hf/W<sub>p</sub> and 2 wt% CVD Hf + 8 wt% powder-mixed Hf/W<sub>p</sub> were tested at high strain rate conditions ( $\approx 10^4$ /sec).

TABLE OF CONTENTS

<u>Section</u>	<u>Title</u>	<u>Page</u>
1.	Introduction	1
2.	Background	2
	2.1 Adiabatic Shear	2
	2.2 Matrix Materials	3
	2.2.1 Hafnium/Tungsten Metallurgy	3
	2.2.2 Titanium/Tungsten Metallurgy	3
3.	Experimental Approach	4
	3.1 Thermodynamic Study	4
	3.2 CVD Powder Coating	4
	3.3 Consolidation	5
	3.4 High Strain Rate Testing	6
	3.5 Characterization	6
4.	Results and Discussion	7
	4.1 Thermodynamic Study	7
	4.2 CVD Powder Coating	7
	4.3 Consolidation	8
	4.4 High Strain Rate Testing	8
5.	Conclusions and Recommendations	10
	References	12

Appendix A. Specifications for M-68 De-Agglomerated Tungsten Powder

Appendix B. Specifications for Annealed Ti(6Al-4V) Alloy

Appendix C. Kaman Sciences High Strain Rate Testing

Appendix D. Caltech High Strain Rate Testing

DTIC QUALITY INSPECTED

<b>Accession For</b>	
NTIS GRA&I	<input checked="" type="checkbox"/>
DTIC TAB	<input type="checkbox"/>
Unannounced	<input type="checkbox"/>
Justification	
By _____	
Distribution/	
Availability Codes	
Dist.	Avail and/or Special
A-1	

## LIST OF FIGURES

<u>Figure</u>	<u>Title</u>	<u>Page</u>
1A.	SEM Micrograph of Ultramet-Coated W/Ni/Fe Composite Consolidated by Ceracon	14
1B.	SEM Micrograph of Commercially Available W/Ni/Fe Composite Consolidated by LPS	14
2A.	SEM Micrograph of Ultramet-Coated W/Ni/Fe Composite Consolidated by Ceracon	15
2B.	SEM Micrograph of Commercially Available W/Ni/Fe Composite Consolidated by LPS	15
3.	Hf-W Phase Diagram	16
4.	Ti-W Phase Diagram	17
5.	Schematic of Ceracon® Consolidation Process	18
6.	Species Concentration vs. Temperature in Zr-I System	19
7.	Experimental Hf:I Ratio vs. Temperature	20
8.	SEM Micrographs of Hafnium-Coated Tungsten Powder	21
9.	EDX Spectrum of Hafnium-Coated Tungsten Powder	22
10.	Composite Optical Micrograph of Hafnium Slug Fracture Region, Showing Possible Shear Bands	23
11.	Composite Optical Micrograph of Hafnium Annulus Fracture Region, With No Shear Bands Evident	24
12.	Optical Micrographs of Hafnium Slug, Showing Both Undeformed Microstructure and Possible Shear Bands	25
13.	Composite Optical Micrograph of Hafnium Slug Fracture Region, Showing Possible Shear Band	26
14.	Composite Optical Micrograph of Hafnium Annulus Fracture Region, Showing Possible Shear Band	27
15.	Optical Micrographs of Hafnium Slug, Showing Both Undeformed Microstructure and Possible Shear Bands	28
16.	Optical Micrographs of Titanium Slug Fracture Region, Showing Possible Shear Bands	29

LIST OF TABLES

<u>Table</u>	<u>Title</u>	<u>Page</u>
I.	Powder Coating Programs at Ultramet	30
II.	Procedures, Reporting Limits, and Precision for Chemical Analysis	31

## 1. INTRODUCTION

This is the final technical report submitted by Ultramet, Pacoima, CA 91331 to the U.S. Army Materials Technology Laboratory, Watertown, MA 02172-0001 under SBIR Phase I contract DAAL04-91-C-0022. The period of this contract was from 5 February to 5 October 1991. The principal investigator was Brian E. Williams, supported by Jacob J. Stiglich Jr. as technical consultant. The AML program manager was Robert J. Dowding.

Extensive research into the mechanisms involved in the success of kinetic energy (KE) penetrator devices has discovered mechanical behavior in depleted uranium (DU) alloys that may be reproduced in more practical ordnance materials. As KE penetrators, tungsten-heavy alloys offer the potential for easier and safer fabrication, handling, and storage compared to DU materials, but the typical ballistic behavior of the tungsten alloys precludes their use for this application. The identification of adiabatic (localized shear) behavior in DU alloys and in other materials such as hafnium and titanium has led to the concept of fabricating a metal composite that incorporates the density and hardness of tungsten, in the form of reinforcing powder particles, with a matrix of a material that exhibits localized shear. In such a composite, the matrix would control the deformation behavior rather than the reinforcement.

The ability to fabricate a metal composed of discrete tungsten particles uniformly surrounded by a matrix of material(s) having vastly different properties is the basis for the powder coating work conducted at Ultramet from 1986 through the present. The benefits of coating individual tungsten powder particles to increase the ductility of tungsten-heavy alloys were shown in previous SBIR Phase I and II programs performed by Ultramet for the Army Materials Technology Laboratory [1,2]. The uniform distribution of a ductile 4.3-wt% nickel/1.7-wt% iron matrix around 12- $\mu\text{m}$  tungsten powder particles led to an increase in flexural strength in consolidated billets as compared to conventional powder-mixed, liquid-phase sintered (LPS) W:7.0Ni:3.0Fe material, while exhibiting an intragranular fracture mode with grain pullout (Figure 1A) rather than purely intergranular (Figure 1B). Figure 2A shows the uniformity of matrix distribution achieved in consolidated Ultramet-coated W:4.3Ni:1.7Fe material, while Figure 2B shows the nonuniform matrix distribution and extensive embrittling tungsten particle-particle contact found in conventional powder mixing/LPS material.

In the present program, Ultramet identified the presence of localized shear bands in monolithic hafnium and the titanium alloy Ti(6Al-4V), and demonstrated the feasibility of coating individual 5.0- $\mu\text{m}$  and 13.6- $\mu\text{m}$  tungsten powder particles with hafnium by chemical vapor deposition (CVD).



## 2. BACKGROUND

### 2.1 Adiabatic Shear

The primary objective of this program was to verify the presence of adiabatic (localized shear) behavior under high strain rate deformation in pure, commercial titanium and hafnium and in hafnium/tungsten powder (Hf/W<sub>p</sub>) and titanium/tungsten powder (Ti/W<sub>p</sub>) composites. Adiabatic behavior has been observed to be important to the penetration capability of depleted uranium (DU) projectiles [3] upon characterizing residual penetrator slugs and the resultant penetration tunnels of various materials, such as DU(½Ti), DU(6Nb), W:7.0Ni/Fe, and W:Ta, recovered from rolled homogeneous armor (RHA) targets. In addition, observations of the penetration of single-crystal tungsten oriented in the [100], [110], and [111] directions (long axis of rod) identified different modes of deformation [4]. [100] penetrators had depths of penetration (DOP) equivalent to DU, suggesting that the [100] material seemed to deform without large-scale plastic deformation, permitting easy material flow away from the penetration interface. This behavior was explained in terms of the favorable slip/cleavage that occurred during the compressive loading of the penetrator material flow without large-scale plastic deformation, and the final shear localization at a favorable angle for easy material flow away from the penetration interface. Penetration tunnel shape and dimensions were also measured while recovering residual penetrator fragments of DU(½Ti), W:7.0Ni/Fe, and the [100], [110], and [111] orientations of pure single-crystal tungsten.

As a result of microstructural analysis of residual DU penetrator fragments recovered from RHA targets, an adiabatic shear mechanism has been observed that appears to be important to the observed increased effectiveness of penetration by DU over tungsten composites [3]. The adiabatic shear mechanism is theorized to permit the DU penetrator to remain "sharper" during penetration compared to a tungsten composite penetrator. The front of the DU penetrator fragments at its interface with the armor, forming an unstable "mushroom" whose "petals" shear off adiabatically, becoming less blunted and thereby presenting a smaller area and imposing a larger maximum stress on the armor. The tungsten composite penetrator, conversely, forms a stable mushroom at its interface with the armor, with the petals shearing off only after a stable (larger) hole diameter is formed. In support of this postulate, smaller and deeper penetration cavities have been observed for DU penetrators as compared to tungsten composite penetrators of equal density impacting at similar velocities and kinetic energies. While velocity and kinetic energy alone do not determine interface pressures, they are, along with similar densities and shapes, sufficient to give initial interface (impact) pressures of similar magnitude, thus lending further credence to the observed results.

Localized shear has been reported to occur most readily in materials that have a low strain hardening rate, low strain rate sensitivity, low thermal conductivity, and a high thermal softening rate, such as alloys of aluminum, titanium, copper, and martensitic and ferritic steels [5]. Localized shear bands were previously considered to be detrimental, as earlier failure of the penetrator material results [3]. However, this material failure has since been correlated with the aforementioned smaller penetration diameter and increased penetration depth.

The identification of adiabatic shear behavior in DU alloys and in other materials such as hafnium and titanium led to the concept of fabricating a metal matrix composite that incorporates the outstanding density and hardness of tungsten, in the form of reinforcing powder particles, with a matrix of a material exhibiting localized shear. In such a composite, the matrix would control the deformation behavior rather than the reinforcement. Although the excellent thermal stability and hardness properties of tungsten are in direct opposition to the properties considered beneficial in DU alloys, the high density and fabricability of tungsten-heavy alloys may be utilized in ordnance applications by coupling the material with a matrix that demonstrates adiabatic shear failure.

## 2.2 Matrix Materials

As noted, both titanium and hafnium are known to exhibit the adiabatic shear phenomenon. Investigating both as potential matrix materials was considered desirable because, while the mechanical behavior of titanium has been better characterized and its adiabatic shear mechanism has been better demonstrated, it has a low density ( $4.5 \text{ g/cm}^3$ ). Hafnium may require more development and characterization as a matrix material, but it has a much more attractive density ( $13.3 \text{ g/cm}^3$ ).

### 2.2.1 Hafnium/Tungsten Metallurgy

Figure 3 shows the Hf-W equilibrium phase diagram [6]. Even though an intermetallic ( $\text{HfW}_2$ ) forms at approximately 67 wt% tungsten, the kinetics of its formation would be rather slow at the temperatures of interest due to the refractory nature of both hafnium and tungsten. With hafnium being deposited at less than  $1500^\circ\text{C}$  ( $2730^\circ\text{F}$ ), the formation of  $\text{HfW}_2$  should thus be suppressed relatively easily. The thermal expansion coefficients of  $\alpha$ -Hf and  $\alpha$ -W are 5.8 and  $4.5 \text{ ppm}/^\circ\text{C}$ , respectively, over the temperature range of interest [7]. The similarity of these CTEs virtually eliminates residual stresses between the hafnium coating and tungsten substrate. Two hafnium phases exist,  $\alpha$  and  $\beta$ , with the transformation temperature being  $1743^\circ\text{C}$  ( $3169^\circ\text{F}$ ), which is well above the deposition temperature range.

### 2.2.2 Titanium/Tungsten Metallurgy

Figure 4 shows the Ti-W equilibrium phase diagram [6]. The formation of the  $\beta$ -Ti/tungsten solid solution, which occurs above  $\approx 740^\circ\text{C}$  ( $1360^\circ\text{F}$ ), must be avoided to the largest extent possible in order to achieve the desired deformation behavior. CVD is an excellent means of accomplishing this, by the coating of each tungsten particle with the titanium matrix while maintaining the solid state. Deposition temperature should be kept at around  $500^\circ\text{C}$  or below to avoid the formation of the  $\beta$ -Ti/W solid solution. Such a relatively low temperature would also serve to minimize stresses caused by thermal expansion mismatch. The thermal expansion coefficients of  $\alpha$ -Ti and  $\alpha$ -W are 9.8 and  $4.5 \text{ ppm}/^\circ\text{C}$ , respectively, over the temperature range of interest [7].

### 3. EXPERIMENTAL APPROACH

The primary objective of this program was to demonstrate that a tungsten-heavy composite material, utilizing either hafnium or titanium as the matrix material, can deform at high strain rates via an adiabatic shear mechanism. Process development efforts focused on coating tungsten powder with hafnium by chemical vapor deposition (CVD), using a fluidized-bed deposition process developed in previous studies [1,2]. High strain rate ( $\approx 10^4$ /sec) shear testing was then performed on consolidated Hf/W<sub>p</sub> composites as well as commercially available monolithic hafnium and titanium alloy (Ti(6Al-4V)) materials, in order to confirm the presence of adiabatic shear in these materials and provide a baseline for comparison with other composite metals derived from coated powders.

#### 3.1 Thermodynamic Study

Preliminary thermodynamic studies for the deposition of hafnium were performed using data for zirconium as a substitute for hafnium. Hafnium and zirconium are chemically similar, sharing many properties such as valence and periodic group, although the higher density of hafnium (13.1 g/cm<sup>3</sup>) compared to that of zirconium (6.49 g/cm<sup>3</sup>) is more desirable for this application. Both are deposited from their respective tetraiodides, HfI<sub>4</sub> and ZrI<sub>4</sub>. The SOLGASMIX-PV computer program [9] was used to evaluate thermodynamic equilibrium in an excess of solid zirconium among the following species: I<sub>(g)</sub>, I<sub>2(g)</sub>, ZrI<sub>(g)</sub>, ZrI<sub>2(g)</sub>, ZrI<sub>3(g)</sub>, ZrI<sub>4(g)</sub>, and Zr<sub>(s)</sub>. The theoretical model based on zirconium was then tested and confirmed using hafnium, establishing the most suitable deposition temperature to be in the 1000-1500°C (1830-2730°F) range.

#### 3.2 CVD Powder Coating

CVD has been used for the deposition of some 400 species [9], the processes for many of which were pioneered by Ultramet personnel. The CVD process has long been successfully utilized for coating particles, such as the production of ultrapure tungsten and niobium spheroids for metallurgical purposes and the cladding of nuclear fuel (UO<sub>2</sub>) particles.

One of the primary advantages of CVD over other plating methods is the extremely high level of purity that may be obtained in the deposit [9]. The majority of impurities in a coated powder batch is due to contamination in the as-received, uncoated substrate powder itself. In the case of deposition on tungsten powder, Ultramet has shown that light-element impurity levels (particularly carbon and oxygen) may be substantially reduced through heat treatment, hydrogen reduction, and/or controlled water vapor treatment of the as-received powder. Carbon levels were reduced by a factor of twelve from the as-received, uncoated powder to the coated, treated powder, and oxygen levels were reduced by a factor of four [2]. Reduction of embrittling impurities can lead to substantial increases in mechanical properties.

Ultramet has been developing fluidized-bed CVD powder coating technology since 1986, largely under SBIR support, although powder coating work is increasingly progressing into the Phase III commercial arena on a small scale [1-2,10-14]. The fluidized-bed CVD process and apparatus developed during the course of this

work are capable of both fluidizing and coating metallic and ceramic particles as small as 5  $\mu\text{m}$  in diameter with a large number of different metal and ceramic materials (see Table I). Batch sizes of up to 1 kg have been produced, and a 5-kg batch reactor is being put into operation. Additionally, a design and cost analysis for a production-oriented reactor is being conducted. This would be a production prototype to be built and operated in any larger-scale commercial applications.

The substrate material for all deposition work was M-68 deagglomerated tungsten powder, procured from GTE Products Corp. (Towanda, PA). This material had previously proved to be an effective substrate for CVD powder coating studies. Prior to coating, it was easily reduced in hydrogen to yield post-coating carbon and oxygen levels of <30 ppm and <150 ppm respectively. The manufacturer's specifications for the M-68 tungsten powder are shown in Appendix A.

In determining the compositions to be investigated, the emphasis was on avoiding chemical/metallurgical interactions between the matrix phase and the tungsten powder particles. It was hoped that if reactions linking the particles to the surrounding matrix could be avoided, the tendency of shear bands to form in the matrix would at least not be degraded by having to interact directly or indirectly with the powder particles. The literature included references to shear band widths on the order of 15-50  $\mu\text{m}$  [15], and metallographic examination of deformed monolithic hafnium and Ti(6Al-4V) at Ultramet gave results consistent with those observations. Compositions were then chosen that provided at least 50-100  $\mu\text{m}$  of matrix phase between adjacent tungsten powder particles, with the aim to provide adequate matrix volume and distribution to permit unimpeded propagation of shear bands by creating the correct conditions in the composites for their formation. W:15 wt% Hf and W:15 wt% Ti compositions were selected for initial evaluation, with the latter subsequently being dropped from the Phase I effort in favor of concentrating solely on hafnium deposition.

A fluidized-bed CVD reactor was designed and fabricated such that powder coating could be conducted at the high temperatures of interest, in batch sizes of  $\approx$ 100 g. Hafnium was then deposited on 100-g batches of 5.0- $\mu\text{m}$  and 13.6- $\mu\text{m}$  tungsten powder by CVD via the thermal decomposition of hafnium tetraiodide ( $\text{HfI}_4$ ) at temperatures ranging from 1000 to 1500°C (1830-2730°F). Although the smaller powder theoretically leads to a superior consolidated product, the degree of agglomeration in the as-received 13.6- $\mu\text{m}$  tungsten powder was far lower than that of the 5.0- $\mu\text{m}$  powder. For this reason, the 13.6- $\mu\text{m}$  material was given greater emphasis. Process development for the deposition of titanium, meanwhile, was left for follow-on work.

### 3.3 Consolidation

The metal-coated powder was consolidated by the Ceracon<sup>®</sup> process, a form of dynamic hot isostatic pressing developed by Ceracon Inc. (Sacramento, CA). This process is illustrated schematically in Figure 5. The Ceracon process utilizes a solid particulate material as the pressure-transmitting medium. The particulate material and the preform compact are first rapidly heated to the same temperature, outside the die. The heated particulate then fills the die, into which the heated compact is inserted. A hydraulic press ram then pressurizes the particulate and consolidates the part. Substantially higher loadings can be achieved by the Ceracon process as compared to conventional hot pressing

techniques; also, consolidation times are far shorter than standard hot isostatic pressing (HIP) or liquid-phase sintering (LPS) methods.

### 3.4 High Strain Rate Testing

High strain rate testing was performed by Kaman Sciences Corp. (Colorado Springs, CO) and by the California Institute of Technology (Caltech) (Pasadena, CA), on commercially available monolithic hafnium and titanium alloy (Ti(6Al-4V)) materials and Ultramet-coated/Ceracon-consolidated Hf/W<sub>p</sub> composites. The manufacturer's specifications for the annealed Ti(6Al-4V) alloy are shown in Appendix B. Strain rates of 10<sup>2</sup>/sec to 10<sup>4</sup>/sec were imposed by a split compression Hopkinson bar apparatus, a technique that had been used successfully in previous studies to evaluate the high strain rate behavior of CVD tungsten [16,17]. The details of the testing procedure, including specimen geometries, are provided in Appendix C (Kaman) and Appendix D (Caltech).

### 3.5 Characterization

Uncoated (as-received) and coated powders were characterized both in-house and externally. In-house analysis included evaluation of coating uniformity and degree of powder agglomeration by optical and scanning electron microscopy (SEM). Energy-dispersive X-ray (EDX) analysis was utilized to determine the presence and distribution of the composite elements, although it was determined that accurate quantitative analysis could not be achieved by this method. Precise analysis of the metal and light element constituents of the coated powder material was performed by Teledyne Wah Chang (Albany, OR). The procedures, reporting limits, and precision limits for the chemical analysis are shown in Table II.

Consolidated billet cross-sections and fracture surfaces were initially evaluated by optical microscopy for low-magnification study. Following the final phase of consolidation and high strain rate testing, the cross-sections and fracture surfaces were subjected to SEM analysis to evaluate matrix distribution and failure mode.

## 4. RESULTS AND DISCUSSION

### 4.1 Thermodynamic Study

As noted, preliminary thermodynamic studies for the deposition of hafnium were performed using data for zirconium as a substitute for hafnium, as much more extensive thermodynamic data is available for zirconium. Hafnium and zirconium are chemically similar, sharing many properties such as valence and periodic group. The SOLGASMIX-PV computer program [8] was used to evaluate thermodynamic equilibrium in an excess of solid zirconium among the following species:  $I_{(g)}$ ,  $I_{2(g)}$ ,  $ZrI_{(g)}$ ,  $ZrI_{2(g)}$ ,  $ZrI_{3(g)}$ ,  $ZrI_{4(g)}$ , and  $Zr_{(s)}$ . A graph of this data (Figure 6) shows  $ZrI_4$  to be the dominant species up to  $\approx 530^\circ\text{C}$  ( $990^\circ\text{F}$ ),  $ZrI_3$  dominant from  $530$ - $760^\circ\text{C}$  ( $990$ - $1400^\circ\text{F}$ ), and  $ZrI_2$  dominant at temperatures above  $760^\circ\text{C}$  ( $1400^\circ\text{F}$ ).

Graphing the metal content of the gas relative to halide content shows a maximum ratio that is characteristic of multiple-valence metals, and indicates the temperature and pressure at which the zirconium content of the gas is maximized. At temperatures above and below this value, zirconium would precipitate from the vapor by decomposition or disproportionation, respectively.

To confirm the theoretical model based on zirconium, the burn rate of hafnium metal in iodine vapor was measured at  $600$ ,  $800$ ,  $900$ , and  $1000^\circ\text{C}$  ( $1110$ ,  $1470$ ,  $1650$ , and  $1830^\circ\text{F}$ ). This was accomplished by evaporating iodine in flowing argon, then passing the iodine vapor over a static bed of heated hafnium metal and measuring the weight loss after 30 minutes of reaction. The results, illustrated in Figure 7, show that at temperatures below  $1000^\circ\text{C}$  ( $1830^\circ\text{F}$ ) the Hf/I ratio remained below 0.25, indicating that kinetic factors, rather than equilibrium, dominate the iodination of hafnium below  $1000^\circ\text{C}$ . The significance of the 0.25 ratio value is related to the fact that the stable compound is  $HfI_4$ .

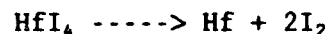
### 4.2 CVD Powder Coating

100-g batches of  $5.0\text{-}\mu\text{m}$  and  $13.6\text{-}\mu\text{m}$  tungsten powder were fluidized and coated with hafnium in the fluidized-bed reactor. Process development of titanium deposition was left for follow-on work, in order to concentrate more fully on hafnium deposition.

The hafnium deposition process began with the *in situ* formation of hafnium tetraiodide ( $HfI_4$ ), the hafnium precursor, via the iodination of hafnium metal chips (99.99% pure) with iodine vapor (99.999% pure) by the following reaction:



The  $HfI_4$  vapor was then transported to the fluidized-bed deposition zone via an argon carrier gas, where it thermally decomposed in accordance with the following reaction to deposit hafnium metal on the tungsten powder substrate:



The heated tungsten powder particles act as nucleation sites for the growth of continuous hafnium films. Figure 8 shows micrographs of hafnium-coated  $5.0\text{-}\mu\text{m}$  and  $13.6\text{-}\mu\text{m}$  tungsten powder, respectively. The presence of hafnium in these

specimens was confirmed by EDX microanalysis, as shown in Figure 9. External analysis by optical emission spectroscopy determined the composition to be W:2.1Hf ( $\pm 0.105\%$ ).

The amount of hafnium deposited was significantly less than the desired 10 wt%, due to difficulties encountered in the mechanics of the reactor itself. The relatively high deposition temperatures (1000-1500°C/1830-2730°F), caused difficulties with regard to deposition on the reactor walls. In addition, this temperature region led to a small degree of sintering if the powder charge was not well-fluidized throughout the entire run. The increased temperature for hafnium deposition, however, is not anticipated to create a tendency for solid solution formation between the hafnium and tungsten. There should be no interaction between the metals even at these temperatures, because residence time for the powder charge is 60 minutes maximum. The difficulties with both reactor wall deposition and sintering may be substantially reduced through the use of a newly designed fluidized-bed reactor.

#### 4.3 Consolidation

Two Hf/W<sub>p</sub> compositions were consolidated by the Ceracon process. Using proprietary process conditions, 1.0" diameter x 0.3" long specimens of the first composition, 2 wt% CVD Hf/W<sub>p</sub>, were consolidated to a density of 18.97 g/cm<sup>3</sup>, which is 99.2% of theoretical. The consolidated material was then delivered to Caltech for Hopkinson bar testing, with test specimens cut by electrodischarge machining (EDM).

1.0" diameter x 0.3" long specimens of the second composition, 2 wt% CVD Hf:8 wt% mixed PM Hf powder/W<sub>p</sub>, were consolidated (again using proprietary process conditions) to a density of 18.15 g/cm<sup>3</sup>, which is 98.5% of theoretical. This material also delivered to Caltech for Hopkinson bar testing. The density of all materials was estimated through water immersion (densitometer). Ultramet has found this method to be typically accurate to  $\pm 0.2\%$ . The oxygen contents of the composite materials were not determined following consolidation.

#### 4.4 High Strain Rate Testing

Kaman performed high strain rate testing on commercially available specimens of annealed titanium alloy (Ti(6Al-4V)) and pure hafnium, with the procedures and results described in Appendix C. Caltech tested Ultramet-coated/Ceracon-consolidated Hf/W<sub>p</sub> composite specimens in compression and shear, as described in Appendix D.

Figures 10-15 are optical micrographs showing the microstructures in various regions of Kaman-tested hafnium specimens. The micrographs reveal areas that appear to have undergone localized deformation, resulting in the formation of shear bands. Similarly, although not as evident, shear bands were found in Kaman-tested Ti(6Al-4V) material, as shown in Figure 16.

The Kaman testing appears to have confirmed the presence of adiabatic shear in the proposed matrix materials, hafnium and titanium, and will provide a baseline for the composite metals derived from coated powders. Pure hafnium specimens exhibited a stress-strain curve that was consistent with plastic flow and failure

by a localized shear mechanism. Two hafnium specimens in compression exhibited a high strain hardening rate.

The Hopkinson bar testing of Hf/W<sub>p</sub> composites at Caltech was designed to expose the composite material to the same strain rate regime that had been used during the testing at Kaman. An advantage of the Caltech testing was that it required much less material, so that more specimens of each composition could be tested. In addition, some specimens of pure hafnium were tested to verify that the testing conditions used at Kaman were recreated.

Details of the Caltech high strain rate experiments are provided in Appendix D, including strain rates and flow stresses for both 2 wt% CVD Hf/W<sub>p</sub> and 2 wt% CVD Hf + 8 wt% mixed PM Hf powder/W<sub>p</sub> composites. The 10 wt% hafnium specimens were more prone to failure than the 2% hafnium (coated powder only) materials. Moreover, the failure of the 10 wt% hafnium specimens was brittle in nature compared to that of the 2 wt% Hf/W<sub>p</sub>. Preliminary micrographic results, shown in Appendix D, indicate poorly bonded and porous regions with much intragranular failure. Consistent with microscopic evidence, the macroscopic failure of the 10 wt% Hf/W<sub>p</sub> specimens was also brittle in nature.



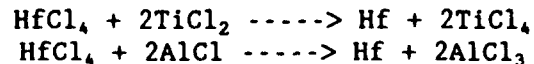
## 5. CONCLUSIONS AND RECOMMENDATIONS

In this program, Ultramet identified the presence of localized shear bands in monolithic hafnium and titanium alloy (Ti(6Al-4V)) materials tested at high strain rates. In addition, the feasibility of coating individual 5.0- $\mu\text{m}$  and 13.6- $\mu\text{m}$  tungsten powder particles with hafnium by CVD was experimentally demonstrated, although the achieved deposition rate and efficiency of the process were not sufficient for fabrication of the desired 10 wt% Hf/ $W_p$  composition.

The accomplishments of both this program and Ultramet's previous work for AMTL, comprising the development of CVD processes for coating tungsten powder, characterization of coated powder, preliminary consolidation studies, and characterization of consolidated billets for physical and mechanical properties, have all contributed to the establishment of a well-defined approach to follow-on work.

The key issues to be examined in future work are process optimization for the deposition of hafnium and titanium coatings on tungsten powder, the amount of each constituent required in the eventual  $W_p$  composite, consolidation of the coated powders, and the degree of post-consolidation mechanical working required to produce high-performance ballistic penetrators, as well as the effects of each on microstructure and high strain rate behavior. The specific technical objectives suggested for such work include the following:

- Modification of existing fluidized-bed reactor designs to allow for continuous processing at the high deposition temperatures of interest, offering the potential for significantly reduced processing costs through a reduction in the amount of labor and precursor material required.
- Integration of the newly developed fluidized bed with optimization of the *in situ* synthesis of the metal iodide precursors ( $\text{HfI}_4$  and  $\text{TiI}_4$ ) for subsequent deposition of hafnium and titanium on 13.6- $\mu\text{m}$  tungsten powder. This study would include further examination of the dissociation and/or thermal decomposition of the metal iodides. The ease of high temperature deposition would be increased through use of the redesigned fluidized bed.
- Simultaneous precursor study to determine the feasibility of depositing hafnium and titanium from their respective chlorides ( $\text{HfCl}_4$  and  $\text{TiCl}_4$ ). These chlorides are extremely stable; however, they are more readily reduced than the iodides, therefore offering the possibility of deposition at a lower temperature.  $\text{HfCl}_4$  may be reduced through the disproportionation of an active metal subhalide. Disproportionation is a process by which a lower valence molecule reacts to form both a zero valence atom and a higher valence molecule. Titanium dichloride ( $\text{TiCl}_2$ ) and aluminum monochloride ( $\text{AlCl}$ ) can be used as reducing agents, as in the following reactions for hafnium deposition from  $\text{HfCl}_4$ :



Contamination of the resultant hafnium deposit with titanium or aluminum is very possible. However, both titanium and aluminum have been shown to exhibit adiabatic shear behavior, so their presence may not be detrimental. The chloride process has the added benefit of utilizing readily available precursors. Organometallic precursors, which offer the possibility of deposition at much lower temperatures, could also be investigated.

- Investigation of various solid-state consolidation techniques, including the Ceracon process and hot isostatic pressing (HIP). Although both of these processes can produce fully dense billets, they differ greatly and produce distinct microstructures.
- Evaluation of the effects of mechanical working of sintered penetrator material through swaging of Hf/W<sub>p</sub> and Ti/W<sub>p</sub> billets derived from consolidated coated powder and subsequent four-point bend testing. The goal would be to achieve 10-15% areal reductions through swaging.
- Characterization of high strain rate ( $\approx 10^4$ /sec) shear deformation mechanisms through Hopkinson bar testing.
- Fabrication and testing of quarter-scale ballistic test specimens (L/D=10) of each optimized composition for evaluation of tensile and ballistic performance.

The proposed program would involve an iterative process, in which the combined effects of CVD powder coating, consolidation, mechanical working, and high strain rate behavior would be evaluated three times during the program. This approach would yield substantial data from which conclusions pertaining to the feasibility of inducing localized shear in tungsten-heavy alloys may be drawn.

Ultramet would like to acknowledge the interest and support of the AMTL program monitor, Robert J. Dowding. Ultramet would also like to extend thanks to Scott Doane and Richard Keefe of Kaman Sciences for their assistance in the area of high strain rate shear testing, and to Dr. G. Ravichandran of Caltech for his efforts in Hopkinson bar compression testing.

## REFERENCES

1. J.G. Sheek, J.J. Stiglich, and J.T. Harding, "Coated Tungsten Powder", Final Report (ULT/TR-87-4831), Contract DAAL02-86-C-0112, Army Materials Technology Laboratory, Watertown, MA, March 1987.
2. B.E. Williams, J.J. Stiglich, and R.B. Kaplan, "Coated Tungsten Powders for Advanced Ordnance Applications, Phase II", Final Report (ULT/TR-91-6821), Contract DAAL04-88-C-0030, Army Materials Technology Laboratory, Watertown, MA, July 1991.
3. L. Magness and T. Ferrand, "Deformation Behavior and its Relationship to the Penetration Performance of High Density KE Penetrator Materials", presented at Army Science Conference, Research Triangle Park, NC, 1990.
4. W. Bruchey, E. Horwath, and P. Kingman, "Orientation Dependence of Deformation and Penetration Behavior of Tungsten Single Crystal Rods", presented at 1991 TMS Annual Meeting, New Orleans, LA, February 1991; published in Tungsten and Tungsten Alloys: Recent Advances, A. Crowson and E. Chen, eds. (The Metallurgical Society, 1991).
5. K. Cho, Y.C. Chi, and J. Duffy, "Microscopic Observations of Adiabatic Shear Bands in Three Different Steels", Technical Report from Materials Research Laboratory, Division of Engineering, Brown University, Providence, RI, to U.S. Army Research Office, Research Triangle Park, NC, September 1988 (ARO Report No. DAAL03-88-K-0015/3).
6. T.B. Massalski, Binary Alloy Phase Diagrams (ASM, Metals Park, OH, 1986).
7. D.T. Vier, "Thermal and Other Properties of Refractories", Technical Report, Program R056, Los Alamos National Laboratories, Los Alamos, NM, March 1975.
8. T. Besmann (Oak Ridge National Laboratory, Oak Ridge, TN), computer code.
9. C.F. Powell, J.H. Oxley, and J.M. Blocher Jr., eds., Vapor Deposition (John Wiley & Sons, New York, 1966).
10. B.E. Williams, J.J. Stiglich, and R.B. Kaplan, "Improved Composite Powder Fabrication", presented at 15th Annual Conference on Composites and Advanced Ceramics, Cocoa Beach, FL, 13-16 January 1991.
11. B.E. Williams, J.J. Stiglich, and R.B. Kaplan, "CVD Coated Tungsten Powder Composites I: Processing and Characterization", presented at 1991 TMS Annual Meeting, New Orleans, LA, 17-21 February 1991; published in Tungsten and Tungsten Alloys: Recent Advances, A. Crowson and E.S. Chen, eds. (The Metallurgical Society, Warrendale, PA, 1991), 95-101.
12. J.J. Stiglich, B.E. Williams, and R.B. Kaplan, "CVD Coated Tungsten Powder Composites II: Fabrication and Properties", presented at 1991 TMS Annual Meeting, New Orleans, LA, 17-21 February 1991; published in Tungsten and Tungsten Alloys: Recent Advances, A. Crowson and E.S. Chen, eds. (The Metallurgical Society, Warrendale, PA, 1991), 103-107.

13. B.E. Williams, J.J. Stiglich, R.B. Kaplan, and R.H. Tuffias, "A Major Advance in Powder Metallurgy", presented at 2nd National Technology Transfer Conference (Technology 2001), San Jose, CA, 3-5 December 1991; published in Conference Proceedings, NASA CP-3136, Vol. 1, 193-202.
14. B.E. Williams, J.J. Stiglich, R.B. Kaplan, and R.H. Tuffias, "The Coating of Powders by Chemical Vapor Deposition", presented at 1991 MTS Fall Meeting, Boston, MA, 2-6 December 1991.
15. S.P. Timothy, "The Structure of Adiabatic Shear Bands in Metals: A Critical Review", Acta Met. 35 (2) (1987), 301-306.
16. J.J. Stiglich and R.B. Kaplan, "High Strain Rate Deformation in CVD Tungsten, Rhenium, and Tantalum", AFATL-TR-89-81 (ULT/TR-89-6796), Air Force Armament Laboratory, Eglin AFB, FL, May 1989.
17. J.J. Stiglich and R.B. Kaplan, "Optimization and Control of Process Parameters for CVD Tungsten Armor-Penetrating Warheads", work in progress under contract F08635-90-C-0282, Air Force Armament Laboratory, Eglin AFB, FL, April 1990 - January 1993.

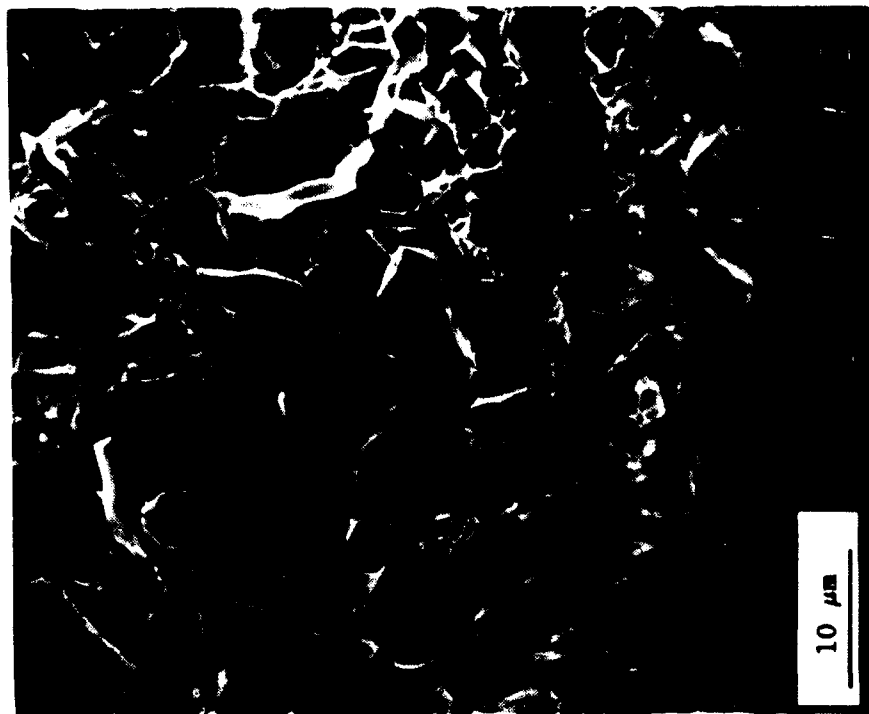
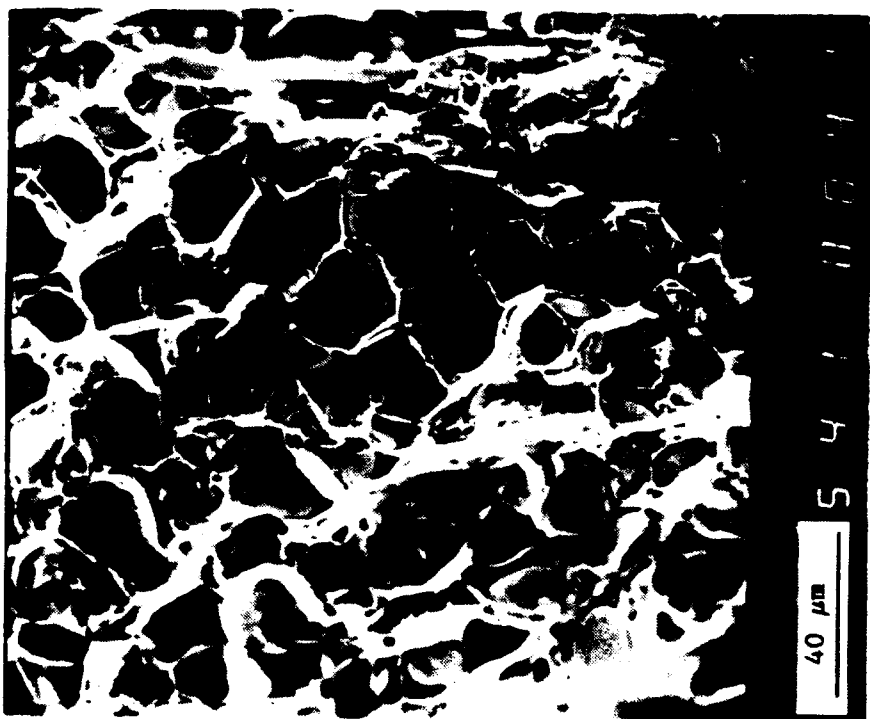


**Figure 1.** **A** (left, 1800x): SEM micrograph of Ultramet W:3.5Ni:1.5Fe composite consolidated by Ceracon, showing significant intragranular failure and grain pullout.  
**B** (right, 540x): SEM micrograph of commercially available W:7.0Ni:3.0Fe composite consolidated by LPS, showing poor matrix distribution and resultant intergranular fracture.

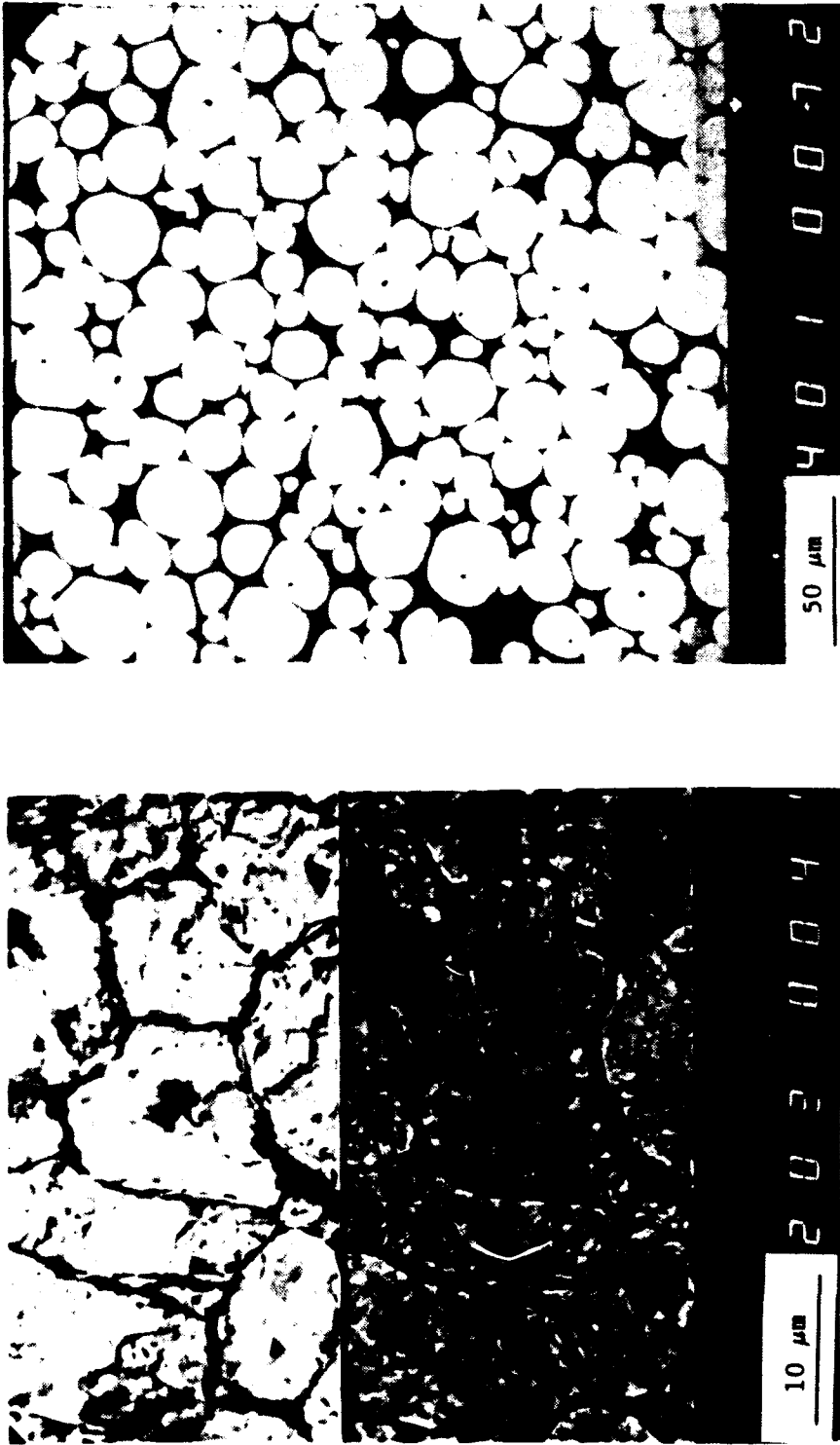


**Figure 2.** A (left, 2000x): SEM micrograph of Ultramet W:3.5Ni:1.5Fe composite consolidated by Ceracon, showing uniformity of matrix distribution  
 B (right, 400x): SEM micrograph of commercially available W:7.0Ni:3.0Fe composite consolidated by LPS, showing non-homogeneous matrix distribution and W-W particle contact.

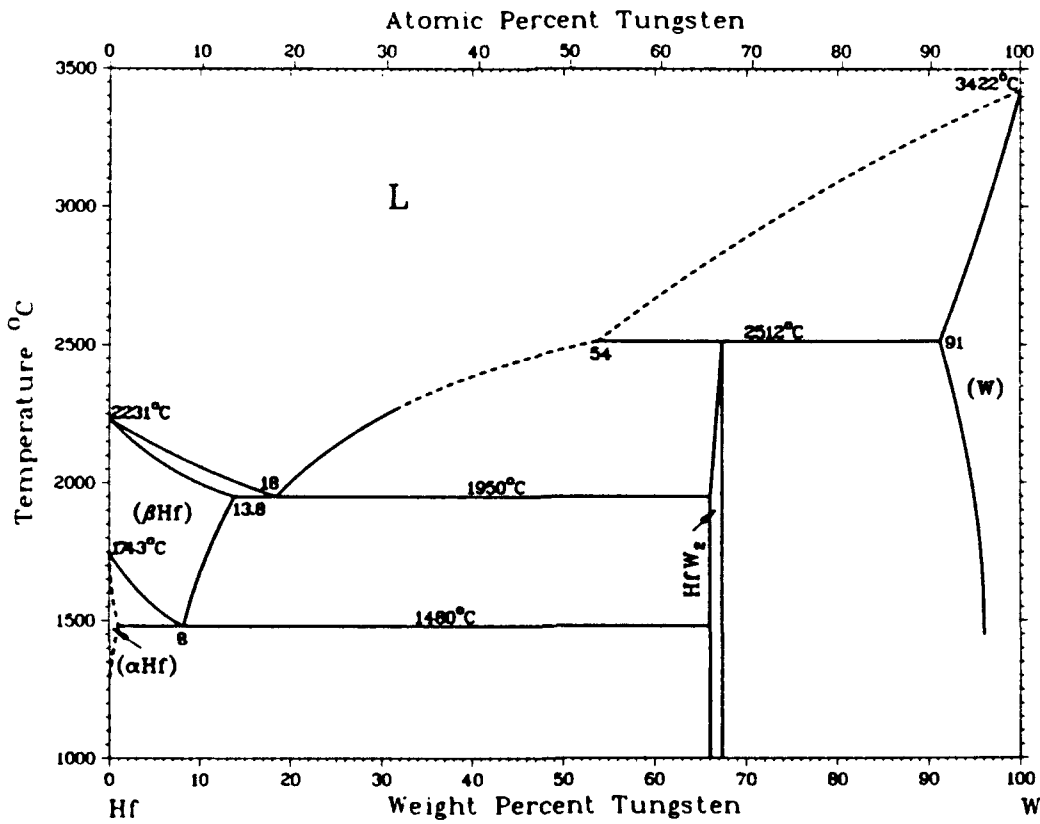
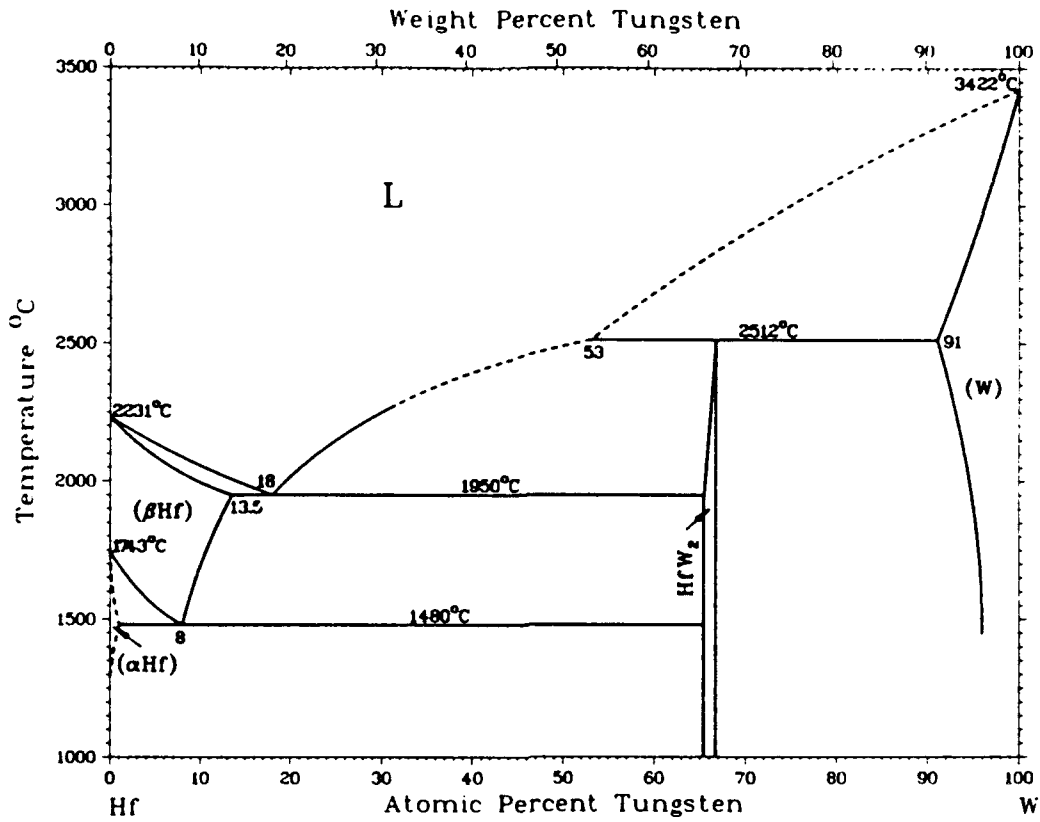


Figure 3. Hf-W phase diagram [6]

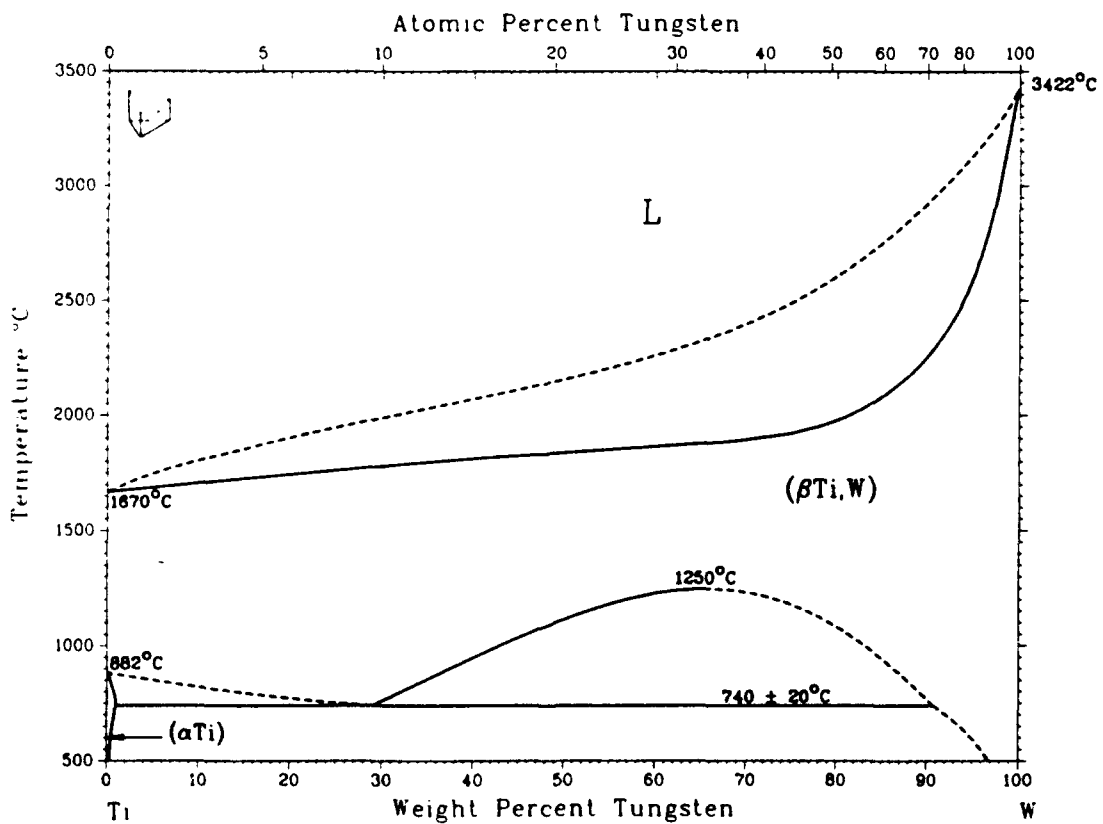
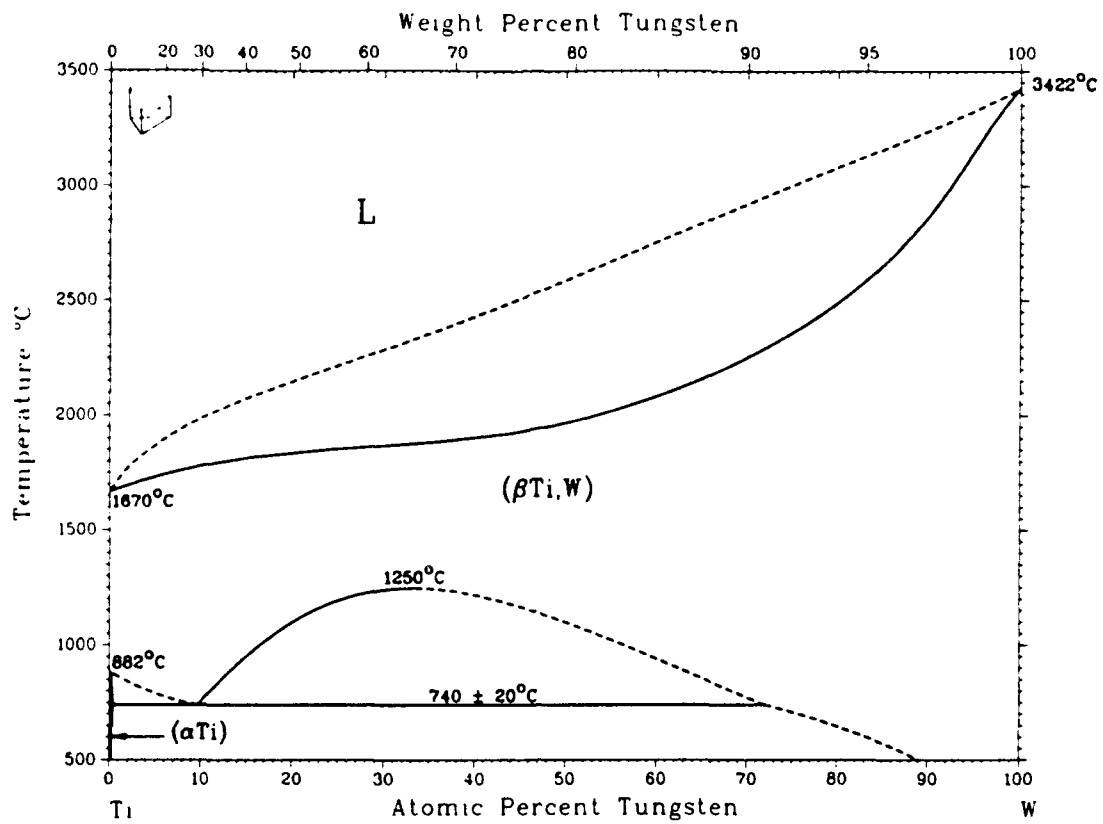


Figure 4. Ti-W phase diagram [6]



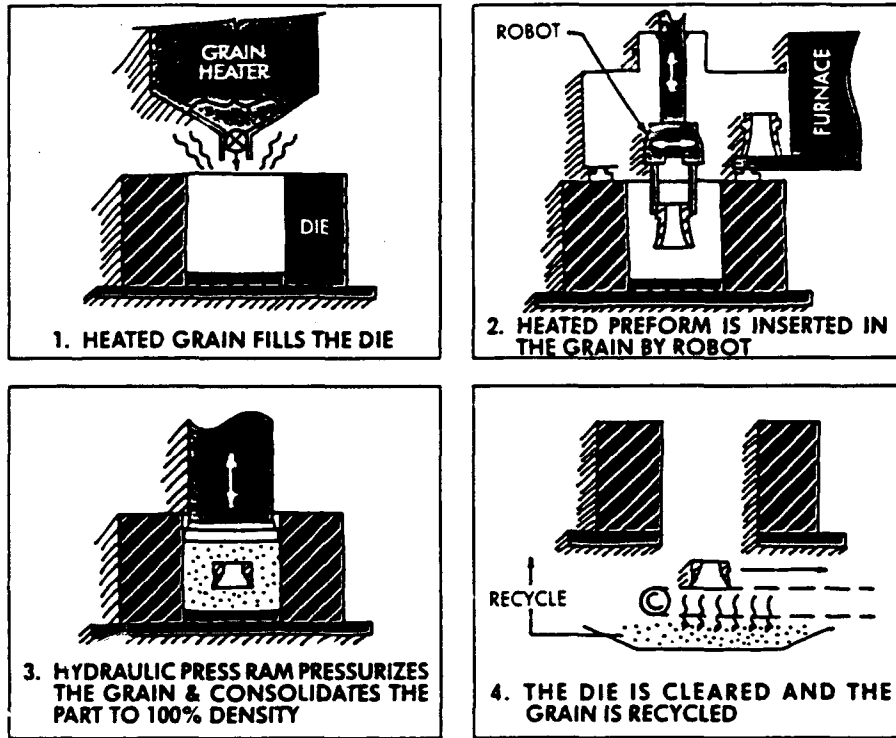


Figure 5. Schematic of Ceracon consolidation process

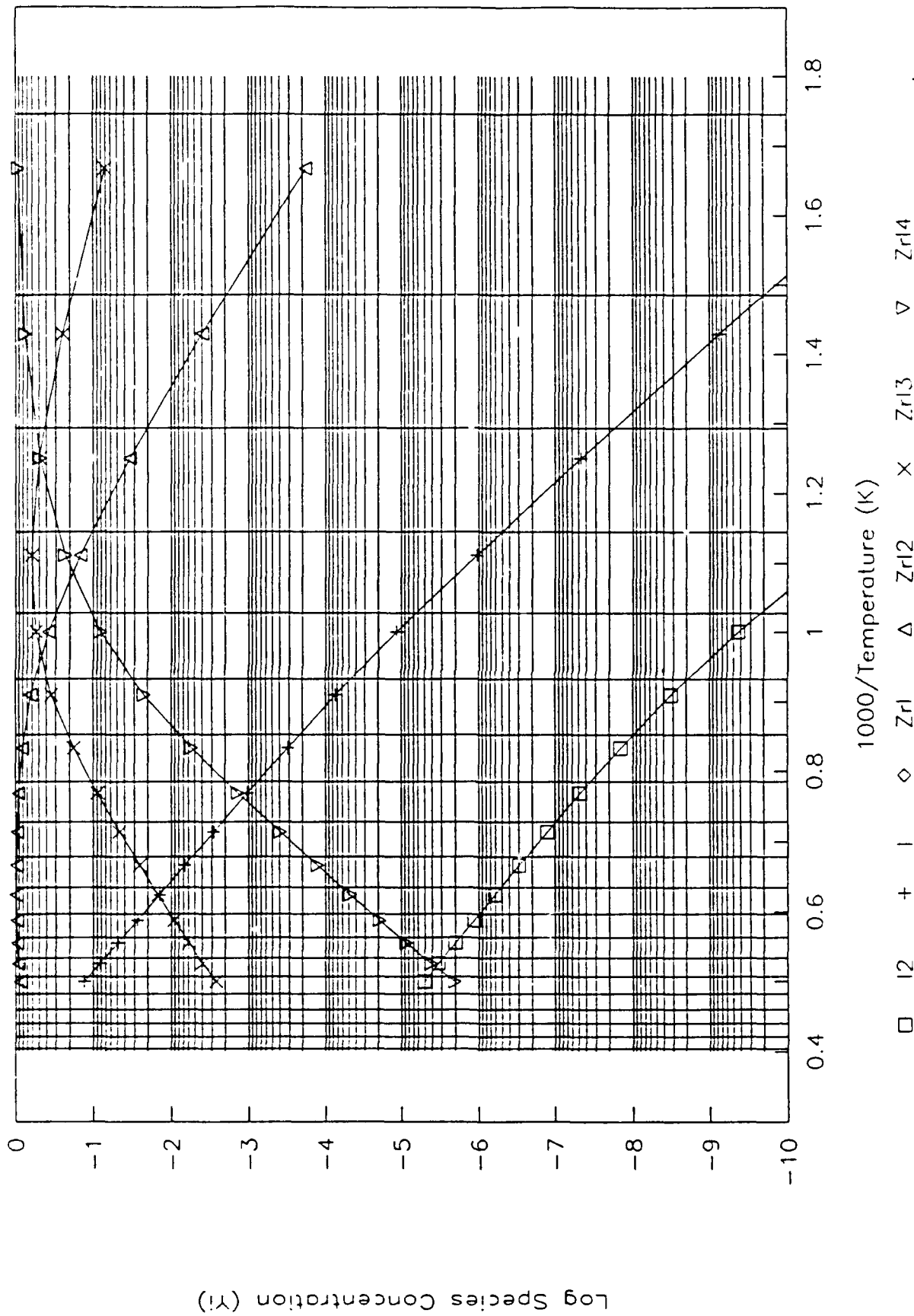


Figure 6. Species concentration vs. temperature in Zr-I thermodynamic system

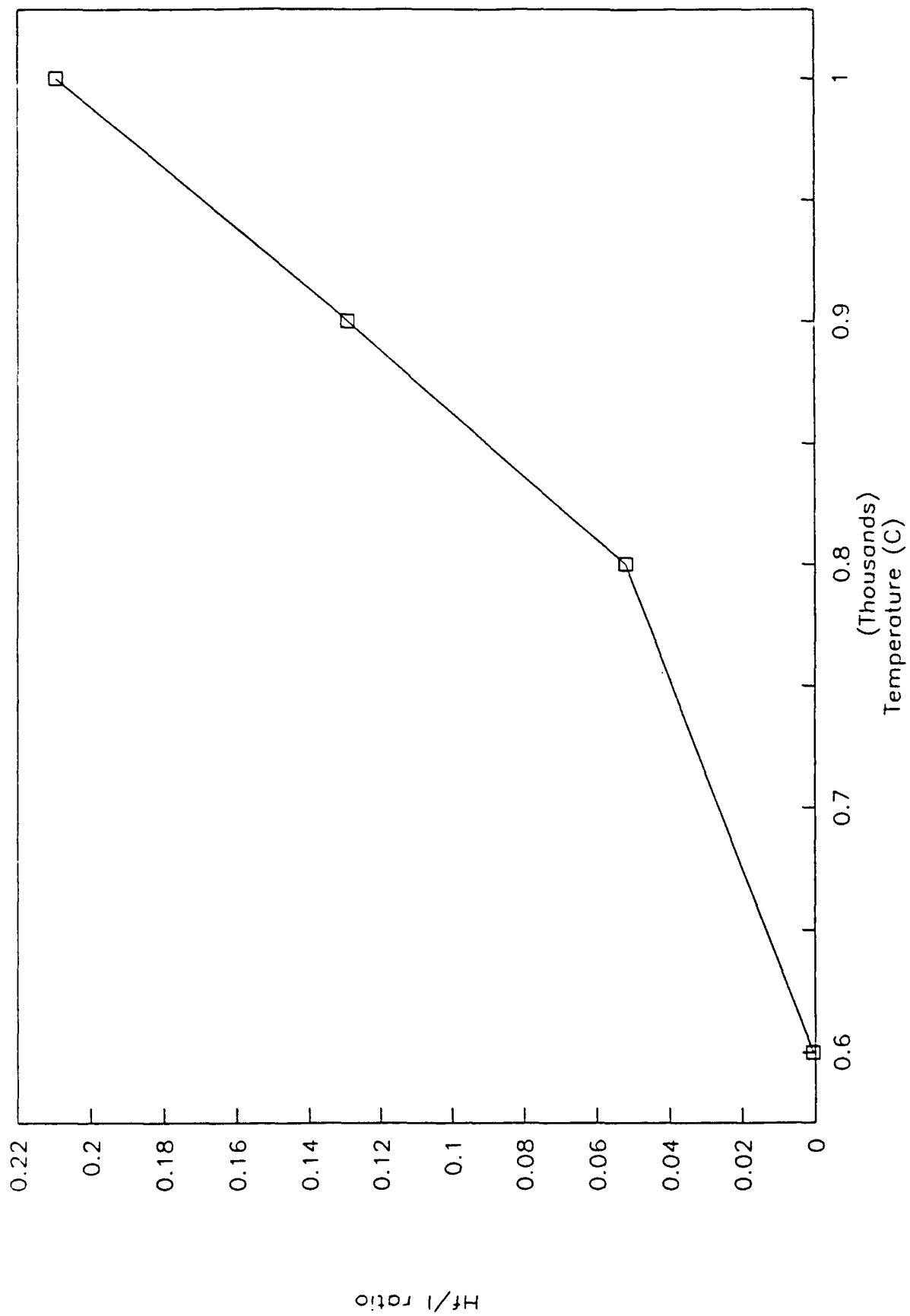


Figure 7. Experimental Hf:I ratio vs. temperature

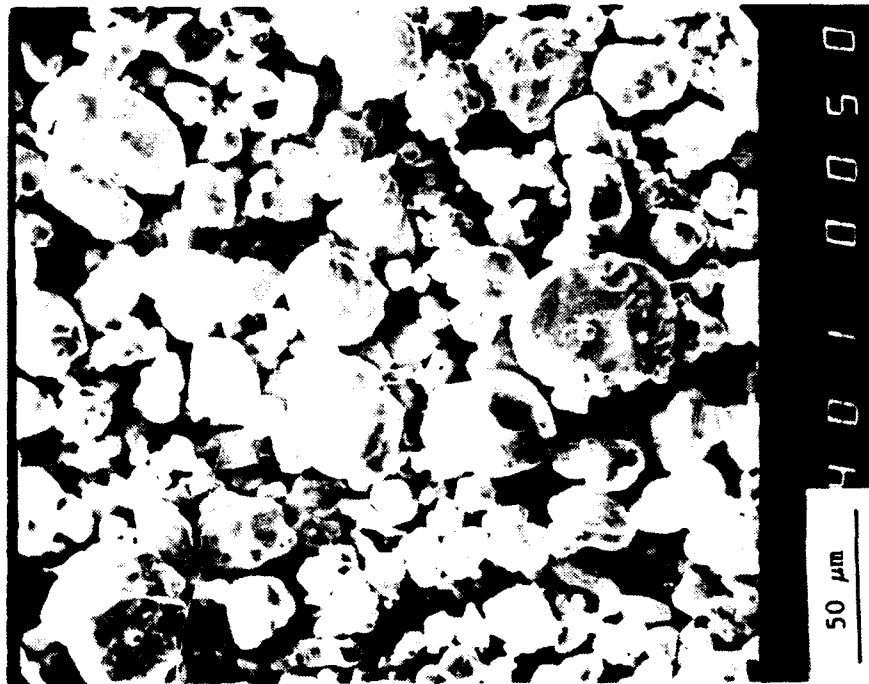
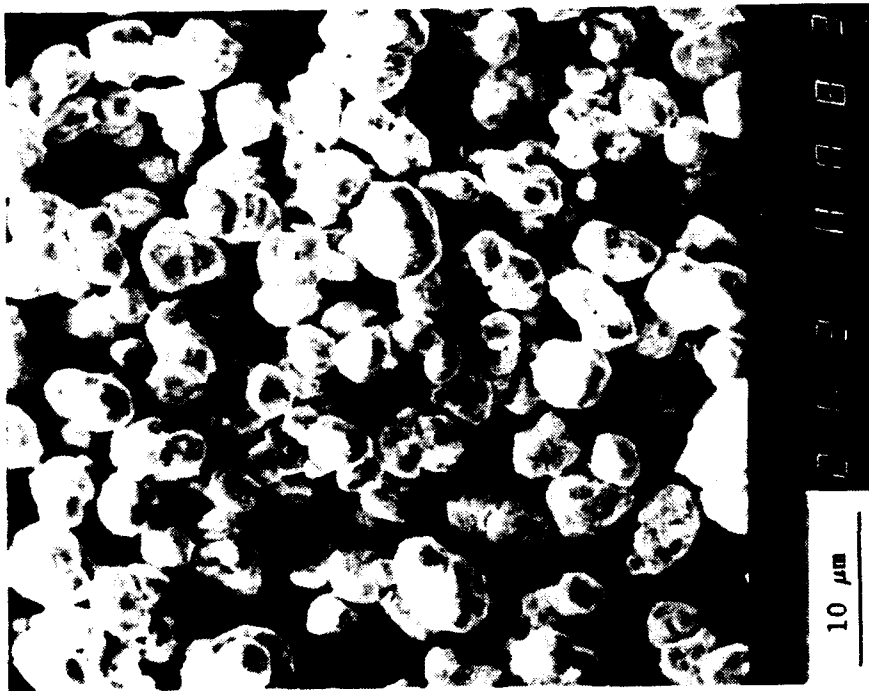
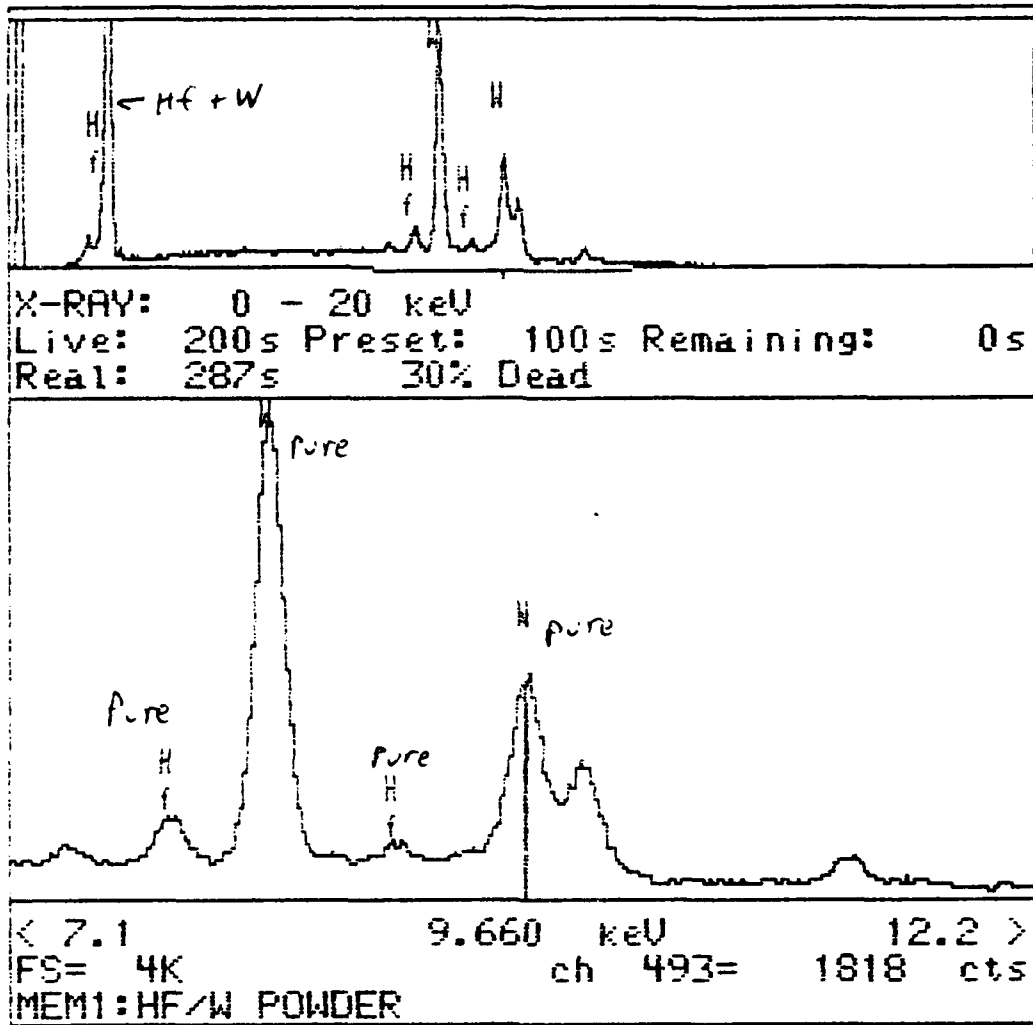


Figure 8. SEM micrographs of hafnium-coated 5.0- $\mu\text{m}$  (left, 2000x) and 13.6- $\mu\text{m}$  (right, 400x) tungsten powder



**Figure 9.** EDX spectrum of hafnium-coated 5.0- $\mu\text{m}$  tungsten powder, showing presence of hafnium. "Pure" notation indicates peaks of hafnium or tungsten only that do not overlap with other elemental peaks. Unmarked, small peaks are unidentifiable and probably represent background "noise" within the equipment.

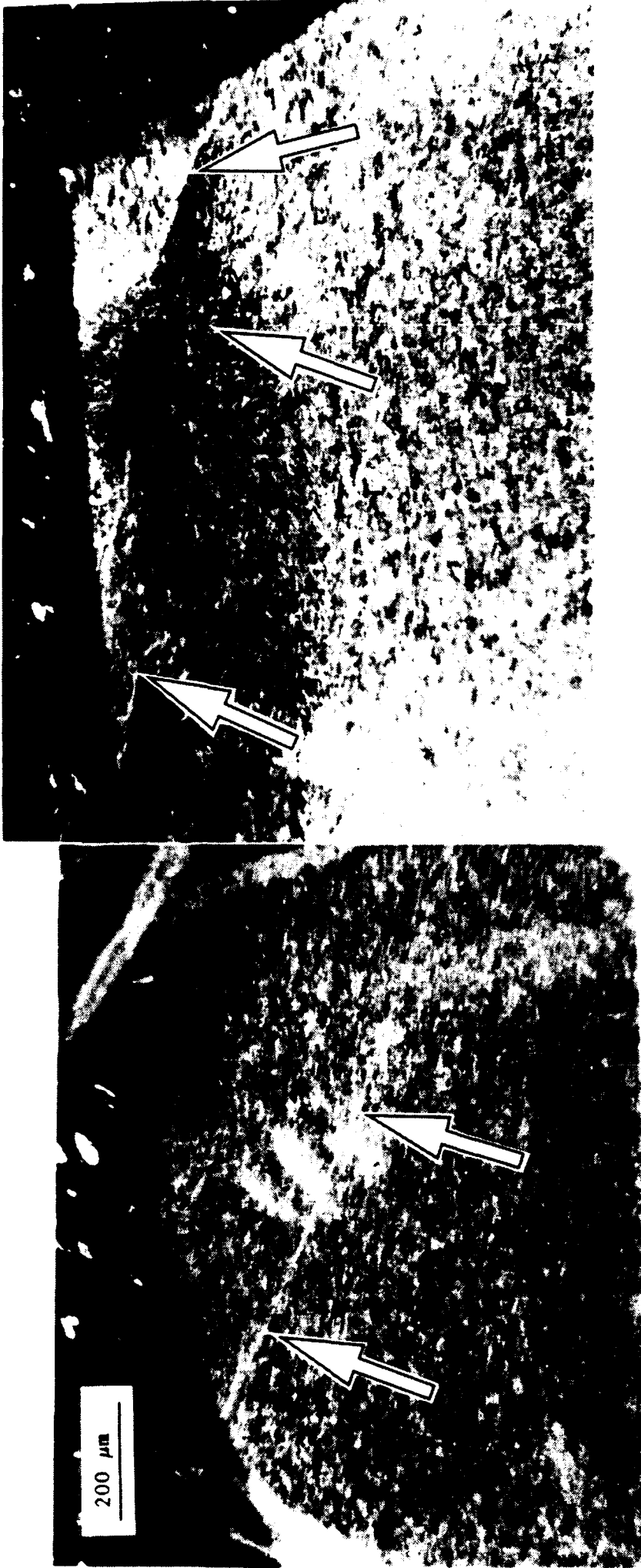


Figure 10. Composite optical micrograph of hafnium slug (fracture region, test #1518), showing possible shear bands (100x, polarized light)

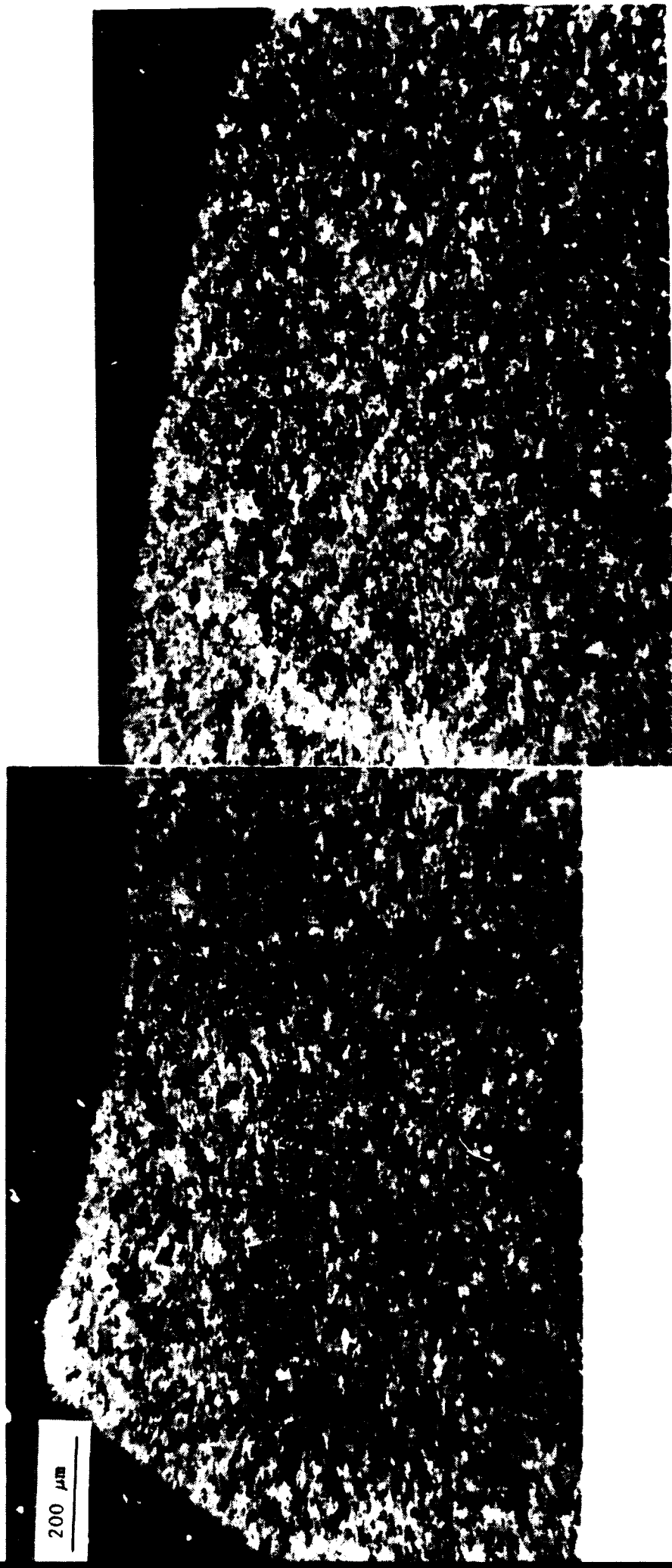


Figure 11. Composite optical micrograph of hafnium annulus (fracture region, test #1518), with no shear bands evident (100x, polarized light)

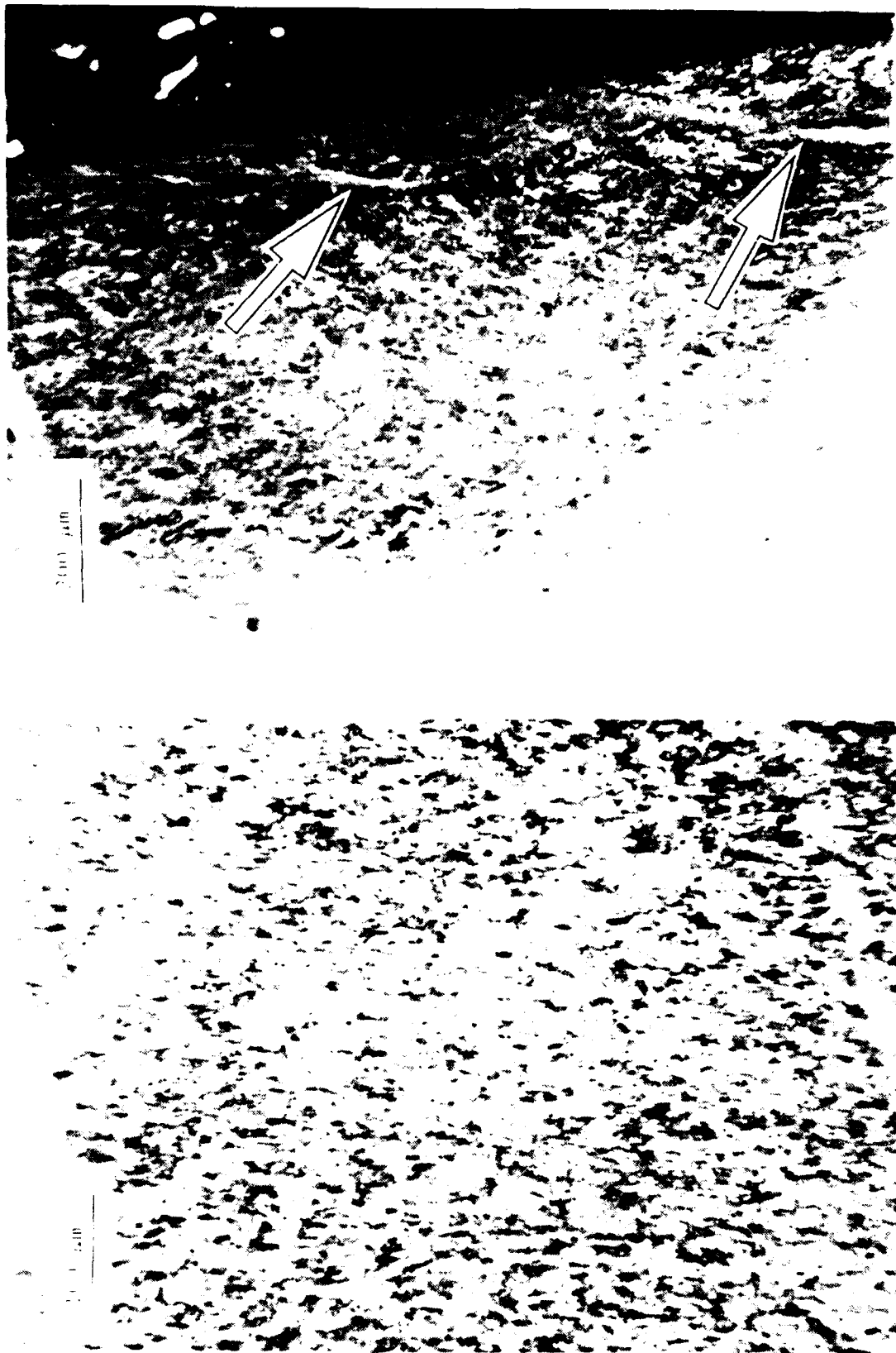


Figure 12. Optical micrographs of hafnium slug (test #1518, polarized light)  
Left: far from fracture region, undeformed microstructure (200x)  
Right: fracture region, showing possible shear bands (100x)





Figure 13. Composite optical micrograph of hafnium slug (fracture region, test #1516), showing possible shear band (100x, polarized light)

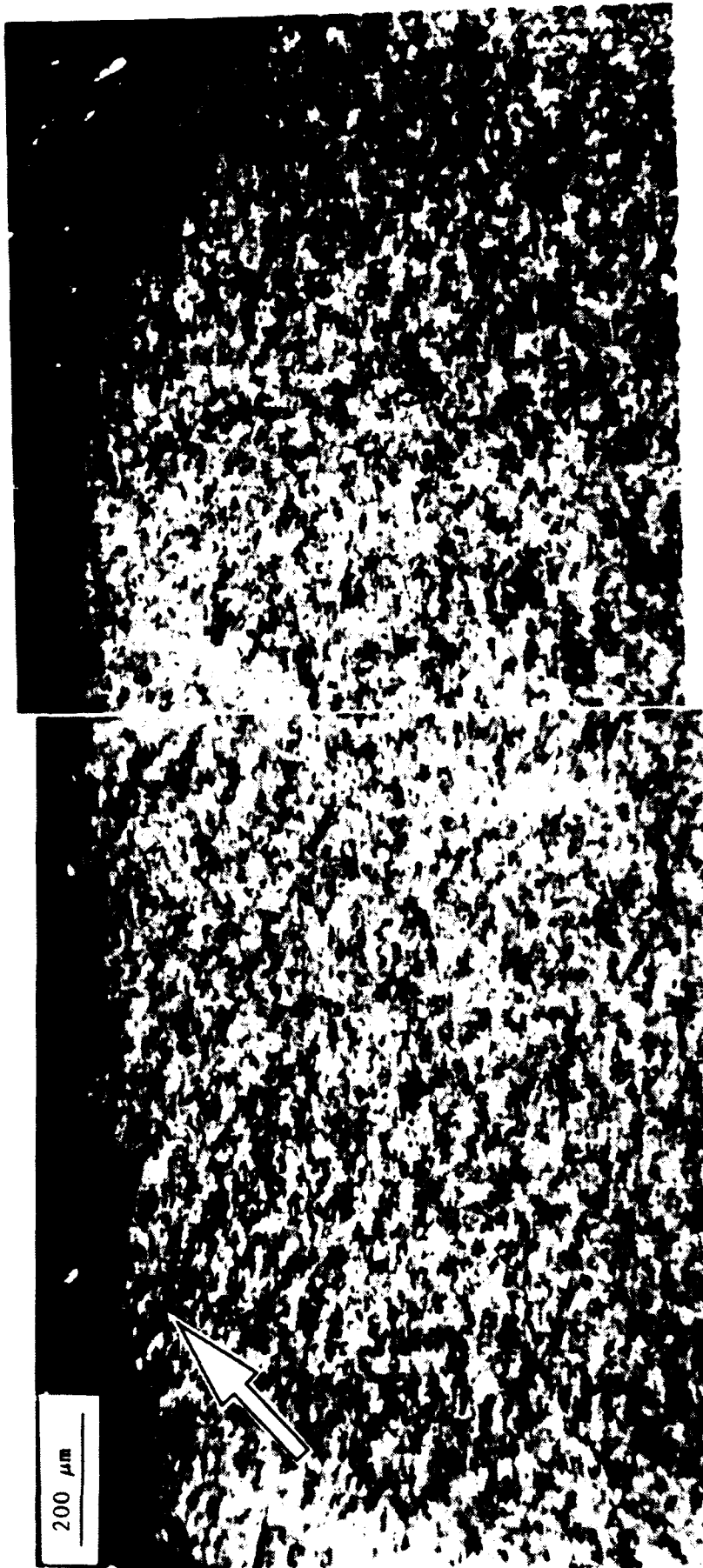


Figure 14. Composite optical micrograph of hafnium annulus (fracture region, test #1516), showing possible shear band (100x, polarized light)

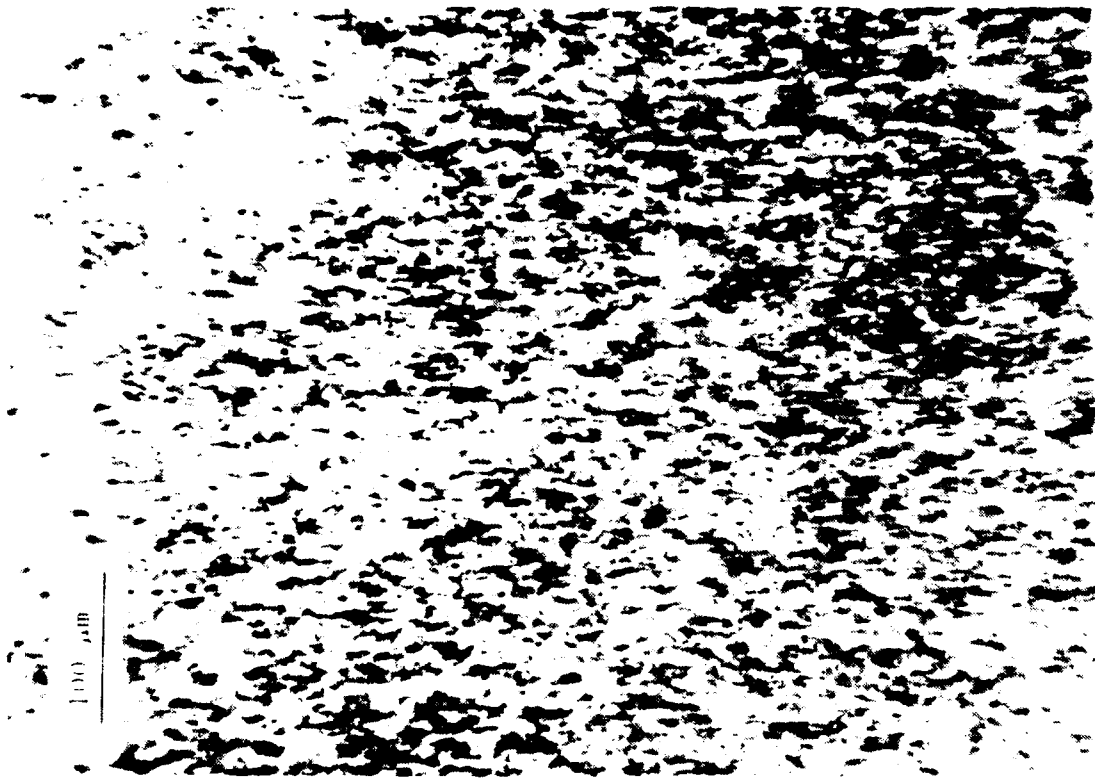


Figure 15. Optical micrographs of hafnium slug (test #1516, polarized light)  
Left: far from fracture region, undeformed microstructure (200x)  
Right: fracture region, showing possible shear bands (100x)

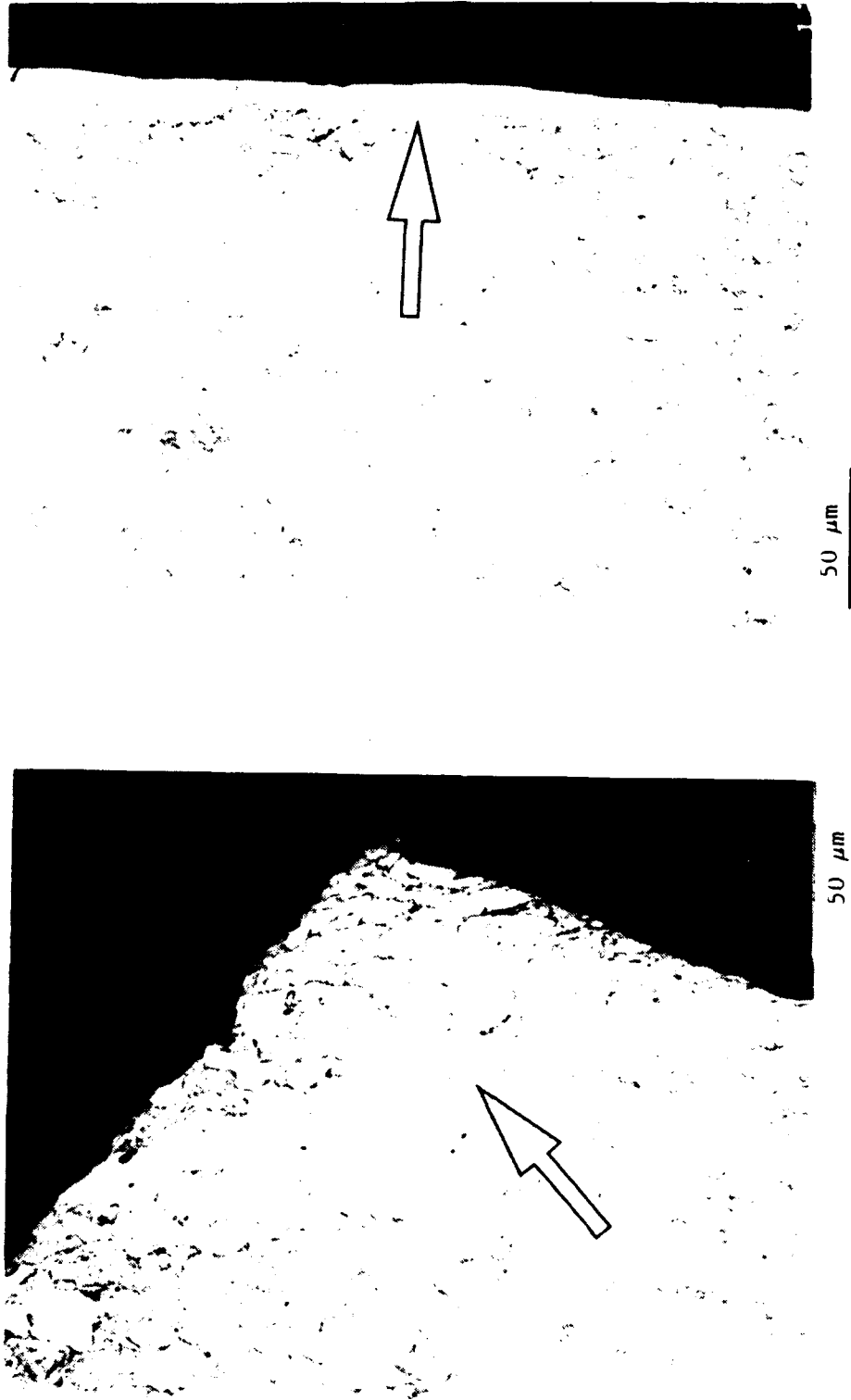


Figure 16. Optical micrographs of titanium (Ti-6Al-4V) slug (fracture region, test #1517), showing possible shear bands (400x, polarized light)

Table I. Powder Coating Programs at Ultramet

Description (coating on powder)	Application
3-4 wt% nickel/1-2 wt% iron on 12- $\mu$ m tungsten	Ordnance
5-50 wt% copper on 100- $\mu$ m AlN	High-conductivity composites
10-30 wt% aluminum on 5- $\mu$ m TiB <sub>2</sub>	Dispersion strengthening
TiB <sub>2</sub> on 5- $\mu$ m aluminum	Dispersion strengthening
80 wt% tungsten on 150- $\mu$ m Al <sub>2</sub> O <sub>3</sub>	Proprietary
10 wt% Al <sub>2</sub> O <sub>3</sub> on 100- $\mu$ m SiC	Ceramic composites
20 wt% titanium on 100- $\mu$ m Al <sub>2</sub> O <sub>3</sub>	Proprietary
5 wt% iron on 100- $\mu$ m WC	Cutting tools
3 wt% cobalt on 10- $\mu$ m WC	Cutting tools
3 wt% iron on 20-500- $\mu$ m diamond	Cutting tools
10-20 wt% hafnium and titanium on 12- $\mu$ m tungsten	Ordnance

Table II. Procedures, Reporting Limits, and Precision for Chemical Analysis

Element	Procedure	Estimated relative precision (%)	Normal low reporting limits (ppm)
Carbon	Combustion/IR: combustion of sample in oxygen, measuring evolved CO <sub>2</sub> by infrared	5	30
Oxygen	IGF/GC: inert gas fusion with gas chromatograph separation of gases using thermal conductivity or infrared readout	5	50
Tungsten	OES: optical emission spectroscopy	5	25
Hafnium	OES	5	25
Titanium	DCPS: direct current plasma source spectroscopy	5	35

**Appendix A.**

**Specifications for M-68 De-Agglomerated Tungsten Powder**

**SYLVANIA**

Chemicals/Metals

GTE Products Corporation  
 Hawes Street  
 Towanda, PA 16848  
 717 265-2121  
 TWX 510 671-4561

Ultramet  
 12173 Montague Street  
 Pacoima CA 91331

Lot No. WA68-409C  
 Sales Order No. T-35399  
 Purchase Order No. 3253  
 Quantity: 4.000 kg.  
 Date: July 12, 1991

## TUNGSTEN POWDER ANALYSIS

Element	RT04000 Limits	Analytical Result	Element	RT04000 Limits	Analytical Result
ppm Al	N/A	<1 ppm	FSSS $\mu$ m	12-14	13.6 $\mu$ m
Ca	N/A	<1 ppm	B.D. g/in3	N/A	146.7 g/in3
Cr	N/A	27 ppm	LOR ppm	N/A	500 ppm
Cu	N/A	<1 ppm	Mo ppm	N/A	14 ppm
Fe	N/A	53 ppm	O2 ppm	275 max	175 ppm
K	N/A	<10 ppm			
Mg	N/A	<1 ppm			
Mn	N/A	1 ppm			
Ni	N/A	41 ppm			
Si	N/A	3 ppm			
Sn	N/A	<1 ppm			
Na	N/A	65 ppm			

The above information covers the physical and chemical analyses of the Tungsten Powder shipped to you.

"Microtrac attached"

Signed By J. J. Penkunas  
 J. J. Penkunas  
 Manager, Quality Control

Apart of GTE Corporation



DATE: 7/ 8/1991

PHYSICAL TESTING LABORATORY MICROTRAC

SAMPLE - WP WA68-409C 10032720

SIZE RANGE	FREQ	CUMM
176.0		100.0
176.0- 125.0	.0	100.0
125.0- 88.0	.0	100.0
88.0- 62.0	.0	100.0
62.0- 44.0	2.3	97.7
44.0- 31.0	10.9	86.8
31.0- 22.0	17.6	69.2
22.0- 16.0	18.5	50.7
16.0- 11.0	19.4	31.3
11.0- 7.8	14.9	16.4
7.8- 5.5	9.9	6.5
5.5- 3.9	4.5	2.0
3.9- 2.8	.9	1.1
2.8- 1.9	.9	.2
1.9- 1.4	.2	.0
1.4	.0	

MEAN 18.43  
SIGMA 11.08  
SKEW .96  
PEAK 3.58

VOLUME MEAN 18.5  
90TH PERCENTILE SIZE 34.8  
MEDIAN 15.8  
10TH PERCENTILE SIZE 6.3

CALC. SPECIFIC SURFACE AREA .496  
UNCALIBRATED SAMPLE VOLUME DATA .184

**Appendix B.**

**Specifications for Annealed Ti(6Al-4V) Alloy**





**Appendix C.**

**Kaman Sciences Test Report**

## TEST PROGRAM TO PRODUCE ADIABATIC SHEAR BANDS IN TITANIUM AND HAFNIUM (monthly progress report)

### 1.0 INTRODUCTION

An adiabatic shear band program was initiated at Kaman Sciences Corporation in support of Ultramet's SBIR contract with the Army Materials Test Laboratory (AMTL). The purpose of the program was to design and conduct tests which produce adiabatic shear bands in titanium and hafnium materials.

### 2.0 BACKGROUND

Adiabatic shear occurs when large amounts of energy are quickly deposited in a localized region in a material, resulting in its thermal softening and the formation of narrow zones of highly displaced material. The deformed zones of material act as a permanent record of the plastic flow which occurred and are referred to as adiabatic shear bands.

### 3.0 APPROACH

Strain rate is a crucial factor in the formation of shear bands since low strain rates allow dissipation of the energy by thermal conduction. Tests must, therefore, be designed to rapidly deposit large amounts of shear strain energy in a small area of the test sample. The tests must also be designed to minimize other deformation mechanisms such as bending stresses.

The tests conducted at Kaman are designed to produce high strain rates in the samples. The strain rates produced in our samples can be calculated by

$$\dot{\epsilon} = \frac{v}{r}$$

where  $\dot{\epsilon}$  is the strain rate, 1/s

$v$  is the velocity, in/s

$r$  is the gap between the central mass and the collar, in

An impact velocity of 2400 in/s (200 ft/s) and a gap of 0.025 inches produces a strain rate of  $1 \times 10^5$  in the test sample. This strain rate deposits large shear strain energy in the test sample.

ABAQUS, a finite element computer code, was used to design the test samples. ABAQUS provided verification that the test design produced maximum shear stress and minimal bending stress in the test sample. The importance of this design was to insure that damage produced in the samples was caused by shear, rather than bending stress.

### 3.0 TEST SAMPLES

Titanium and hafnium bar stock was provided to Kaman by Ultramet. The titanium bar was 1.5 inches in diameter, while the hafnium bar stock was a smaller 1.2 inch diameter. Kaman fabricated the raw bar stock into the test sample geometry.

The test sample and test geometry of each material is shown in Figure 1 and Figure 2. As shown in these figures, two test geometries were employed for each material. The distinguishing feature of the two geometries was the 30° and 45° angle of the notch cut in the test samples. The purpose of the notch was to produce pure shear stress in the test samples.

### 4.0 TEST TECHNIQUE

Kaman used its gas gun facility to launch a projectile carrying the test sample. The test sample, clamped by an annular collar fabricated from Vascomax, is driven into a stop. The collar quickly stops upon striking the stop while the central mass of the test specimen continues. Since the gap between the central mass and the collar is small, the test technique rapidly deposits a high level of shear energy in an extremely small area of the sample. This approach addresses

each critical issue necessary to produce adiabatic shear bands.

#### 4.0 TEST RESULTS

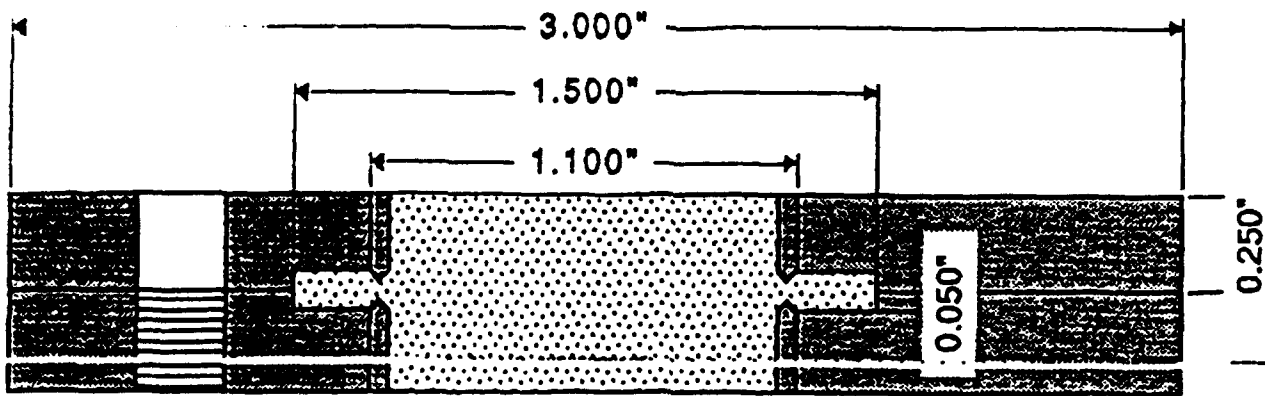
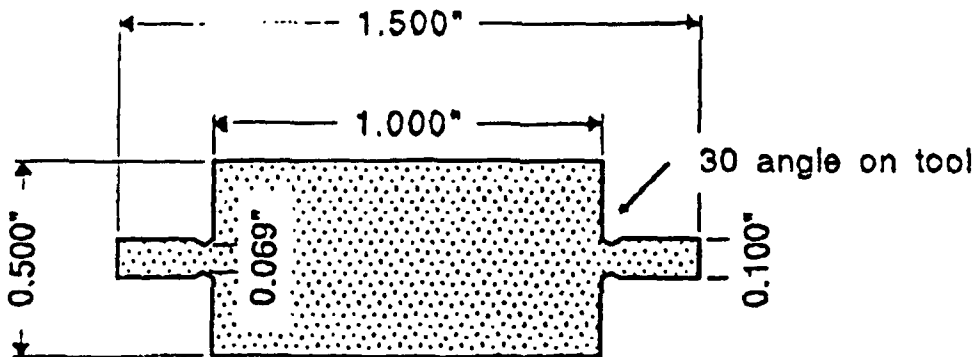
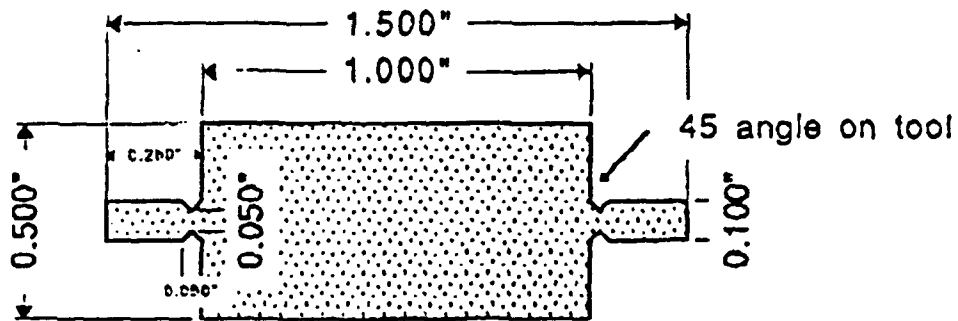
Four adiabatic shear tests were conducted on titanium and hafnium samples. Test parameters associated with each shot are listed in Table 1.

Adiabatic Shear Band Shot Summary				
Shot Number	Sample Material	Overall Sample Dia. (inch)	Notch Angle (deg)	Impact Velocity (ft/s)
1515	Ti	1.5	45	204.7
1516	Hf	1.2	45	213.2
1517	Ti	1.5	30	207.0
1518	Hf	1.2	30	231.0

The four tested samples have been sectioned by Kaman and sent to Ultramet for metallurgical analysis. Initial examinations suggest the hafnium samples may have exhibited adiabatic shear, while the titanium samples did not.



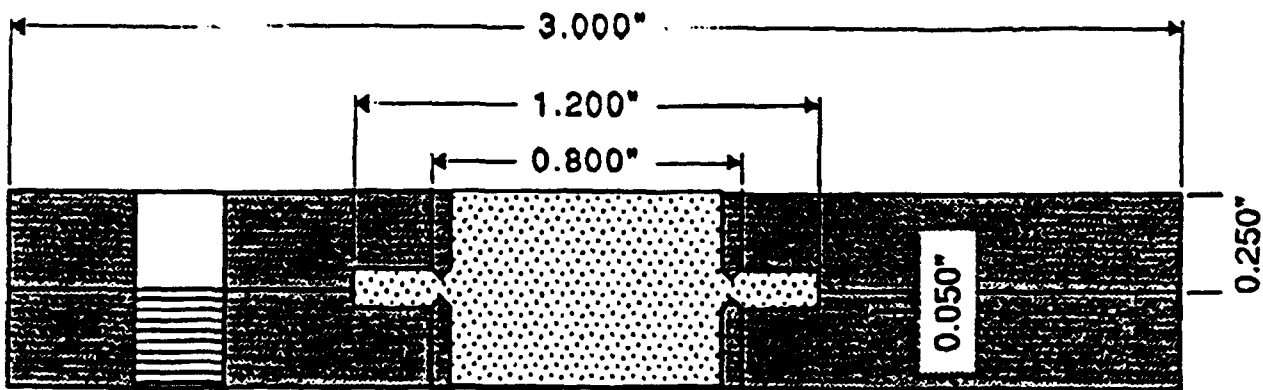
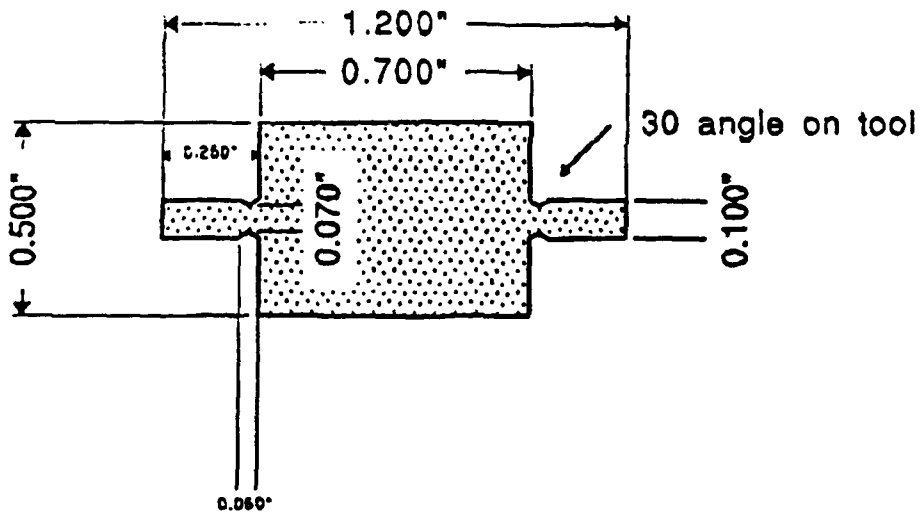
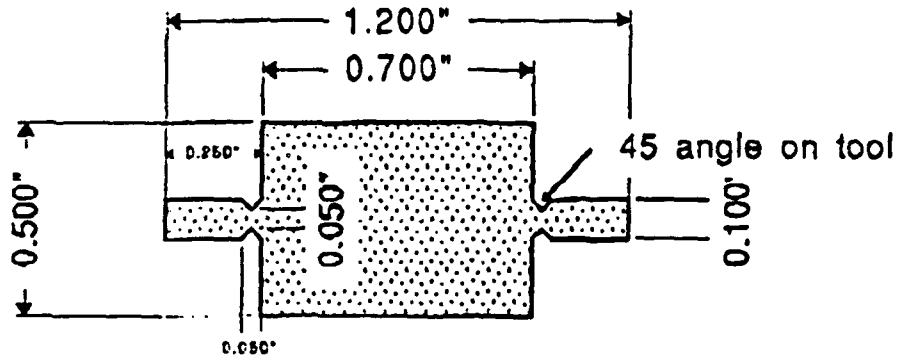
### 2nd Generation Adiabatic Shear Samples Titanium Samples and VASCOMAX Clamp Scale: 2X



↑ tap for 1/4-20, 6 places on 60 degree hole pattern.....

### 2nd Generation Adiabatic Shear Samples Hafnium Samples and VASCOMAX Clamp

Scale: 2X



tap for 1/4-20, 6 places on 60 degree hole pattern

c.050"

**Appendix D.**  
**Caltech Test Report**

GRADUATE AERONAUTICAL LABORATORIES  
CALIFORNIA INSTITUTE of TECHNOLOGY  
PASADENA, CALIFORNIA 91125

FIRESTONE FLIGHT SCIENCES  
LABORATORY

Mail Stop: 105-50  
Telephone: (818) 356-4525

February 20, 1992

Mr. Brian Williams  
ULTRAMET  
12173 Montague Street  
Pacoima, California 91331

Dear Brian:

We have completed the split Hopkinson bar experiments on the W/2%Hf and the W/10%Hf composite specimens provided by you. These experiments were performed by Dr. Subhash Ghatuparthi, Research Fellow at Caltech using our High-Strain-Rate facilities. I am enclosing a summary of the results on the tungsten composites. From these preliminary experiments, it appears that the W/2%Hf material may be more promising for potential applications. If you have any questions, please do not hesitate to contact me.

Sincerely yours,



G. Ravichandran  
Assistant Professor, Aeronautics

Enclosure

cc: Dr. S. Ghatuparthi

# High Strain Rate Behavior of Tungsten-Hafnium Composites

## 1. INTRODUCTION

This report provides a summary of results on high strain rate behavior of tungsten-hafnium composites provided by Ultramet. The preliminary results provided here were obtained using a split Hopkinson pressure bar at the Graduate Aeronautical Laboratories in the California Institute of Technology. The fracture surfaces were examined using a scanning electron microscope.

## 2. MATERIAL

The materials that were tested include a W/2%Hf and a W/10%Hf tungsten composites. Ultrasonic wave velocity measurements were carried out to determine the wave velocities in the samples using a Panametrics ultrasonic analyzer together with longitudinal and shear wave transducers and a high sampling rate (1 GSa/s) digital oscilloscope. The wave velocities were used to determine the bulk elastic properties. The physical properties for the two compositions mentioned above and pure tungsten are shown in Table I.

Table I: Physical Properties of Tungsten/Hafnium Composites

Material		W/2%Hf	W/10%Hf	W
Relative Density		18.50	17.44	19.30
Longitudinal Wave Speed	ft/s	15,910	16,533	17,300
Shear Wave Speed	ft/s	8,960	9,290	9,500
Young's Modulus, E	Mpsi	50	51	60
Shear Modulus, G	Mpsi	19.8	20.1	23
Poisson's Ratio		0.27	0.26	0.29

## 3. EXPERIMENTS

### 3.1. Split Hopkinson Pressure Bar

A high strain rate technique that is commonly used in the characterization of ductile metals at high strain rates is the split Hopkinson pressure bar (SHPB) (also referred to as the Kolsky pressure bar). The concept originally developed by Kolsky, has found widespread applications in testing ductile metals at high strain rates of up to  $10^4 \text{ s}^{-1}$ .

A schematic of the basic SHPB is shown in Fig. 1. When the striker bar impacts the incident bar at a given velocity, an elastic compressive pulse (typical rise times of 10-20  $\mu\text{s}$ ) propagates along the incident bar. The pulse duration equals the round-trip time of an elastic longitudinal bar wave in the striker bar. When the pulse reaches the specimen which is placed between the incident bar and the transmission bar (see Fig.1), part of the pulse is reflected back and the remaining part

is transmitted through the specimen to the transmission bar. The strain gages provide time-resolved measures of the signals in the incident and the transmission bars. From the reflected signal the axial strain in the specimen is estimated, and the transmitted pulse provides a measure of the axial stress in the specimen.

One dimensional calculations show that the strain rate  $\dot{\epsilon}$  in the specimen can be estimated using,

$$\dot{\epsilon} = -\frac{2c_0}{l} \epsilon_r \quad (1)$$

where  $l$  is the original length of the specimen,  $\epsilon_r$  is the time-dependent reflected strain, and  $c_0$  is the longitudinal bar wave velocity in the incident bar which is given by

$$c_0 = \sqrt{\frac{E}{\rho}} \quad (2)$$

where  $E$  is the Young's modulus and  $\rho$  is the mass density of the bar material. The axial stress  $\sigma$  in the specimen is estimated from

$$\sigma = \frac{A_0}{A_s} E \epsilon_r \quad (3)$$

where  $A_s$  is the cross-sectional area of the specimen, and  $\epsilon_r$  is the time-dependent strain in the transmission bar of area  $A_0$ . All the foregoing calculations are based on the assumption that the specimen undergoes homogeneous deformation.

### 3.2. Experimental Facility

The experiments were conducted in a split Hopkinson pressure bar facility at the Graduate Aeronautical Laboratories at Caltech. The SHPB consist of a light gas gun for propelling the striker bars, the incident bar, the transmission bar, and a momentum stopper. The pressure bars are each 4 feet long and 3/4 in diameter, are made of high strength maraging steel. The striker bars are also made of the same material and same diameter as the pressure bars. The striker bars range in lengths from 4 to 12 inches. The uniaxial yield strength of the bars is approximately 350 ksi. The momentum stopper consists of a momentum trap bar and a shock absorber. The momentum trap bar which is in contact with the transmission bar during the experiment is made of maraging steel and is 18 inches in length. The transmitted compressive pulse upon reaching the interface between the transmitter bar and the momentum trap continues to propagate in to the momentum trap. This compressive pulse in the momentum trap reflects as a tensile pulse from its free surface and upon reaching its interface with the transmission bar causes it to unload and separate, thus carrying away the momentum in the transmitted pulse. Thus the specimen is not subjected to repetitive loadings due to reflections within the transmission bar. This facilitates the recovery of specimens for further observations. The strain gages that are used on the bars have resistances of

1000  $\Omega$  and are connected to four arm Wheatstone bridges with temperature compensation. The excitation voltage applied to the bridge is 30.0 Volts and no pre-amplifiers or filters are used on the signals from the bridge. The strain gage signals are recorded directly on a four channel Series 400 Nicolet digital oscilloscope (sampling rate of 10 MSa/s) and are then analyzed using equations (1) and (3).

### 3.3. Results

Five specimens from each composition were tested at strain rates ranging from 350/s to 3,600/s. The results are summarized in Figures 2 and 3. Table II provides a summary of strain rates and flow stresses from the experiments shown in these figures. Figures 2 (a)-(f) summarize the results obtained from experiments on the 2%Hf material. Figures 3 (a)-(e) summarize the results from experiments on the 10%Hf material.

Table II: Summary of Preliminary Experimental Results

Material	Experiment	Nominal Strain Rate $s^{-1}$	Flow Stress, $\sigma_f@5\%$ ksi
W/2Hf	W-2Hf-3-Load 1	350	250
	W-2Hf-3-Load 2	650	260
	W-2Hf-4	2000	275
	W-2Hf-2	2500	280
	W-2Hf-5	3600	295
W/10Hf	W-10Hf-3	750	275
	W-10Hf-1	1700	280
	W-10Hf-4	2000	290
	W-10Hf-2	2200	280
	W-10Hf-5	3000	300

The W/2%Hf material deforms plastically and appears to be fairly rate sensitive. Most of the specimens were recovered without any visible failure. The flow stress levels achieved in the samples are about 300 ksi and the maximum strains achieved in these specimens was about 16%. The W/10%Hf material appears to be less rate sensitive than the W/2%Hf material but the flow stress and maximum strains achieved were approximately the same as the W/2%Hf samples. However, the W/10%Hf samples failed completely upon reaching the maximum strain in a brittle failure mode, i.e. axial splitting. The maximum strains and the flow stress levels achieved in these experimental W/Hf alloys are comparable to the conventional liquid phase sintered WHA (e.g. W/Ni-Fe) alloys.

From these preliminary results, the W/2%Hf material show promise and might be able to undergo further plastic deformation through the flow of hafnium phase at the grain boundaries and is corroborated by the electron micrographs of the failure surfaces.

#### 4. FAILURE MODES

The fracture surfaces from the failed specimens were examined using scanning electron microscopy to identify the failure modes associated with high strain rate deformation of tungsten-hafnium composite samples. Microscopic observations revealed the following distinct failure modes for the two compositions of specimens: (i) mostly cleavage (transgranular) failure in W/2Hf accompanied by some ductile tearing at grain boundaries and (ii) multiple axial splitting, with predominantly intergranular failure in W/10Hf specimens together with cleavage of some tungsten particles.

Figures 4 (a) and (b) are the secondary and back scattered scanning electron micrographs of the planar fractured surface from W/2Hf composition. These micrographs reveal the faceted fracture surface and indicate that the failure occurs by transgranular cleavage. Also the irregular surface observed indicate that there may be ductile tearing associated with hafnium coated on the grains. Figures 5(a) and 5(b) show secondary images of W/10%Hf fracture surfaces. These micrographs reveal that the failure is predominantly intragranular (grain boundary failure) which is can be deduced from the irregular fracture surfaces but at the same time, there appears to be a small fraction of grains that have undergone cleavage.

The issues related to strain rate sensitivity, possibility of localized shear in W/Hf alloys and associated micromechanisms of deformation and failure deserve further detailed study. These can be accomplished through controlled high strain rate experiments as the ones described here and analytical (transmission) electron microscopy.



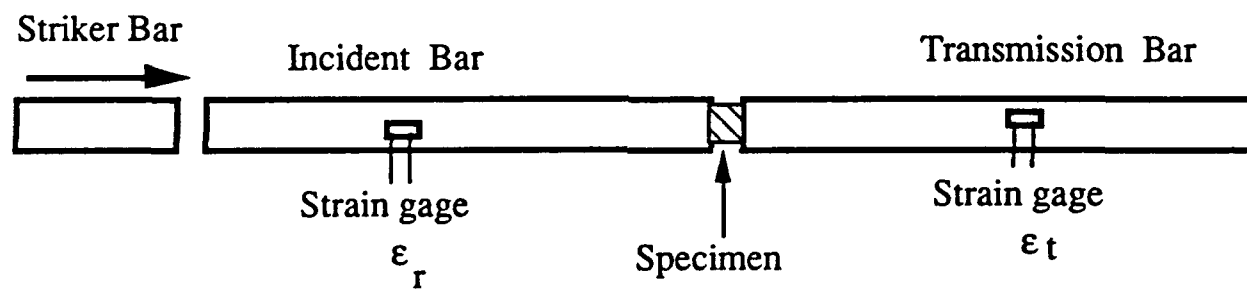


Figure 1: Schematic of a Split Hopkinson (Kolsky) Pressure Bar.

W2HF1  
L = 0.1279", D = 0.2499"; Strain Rate = 1900/s

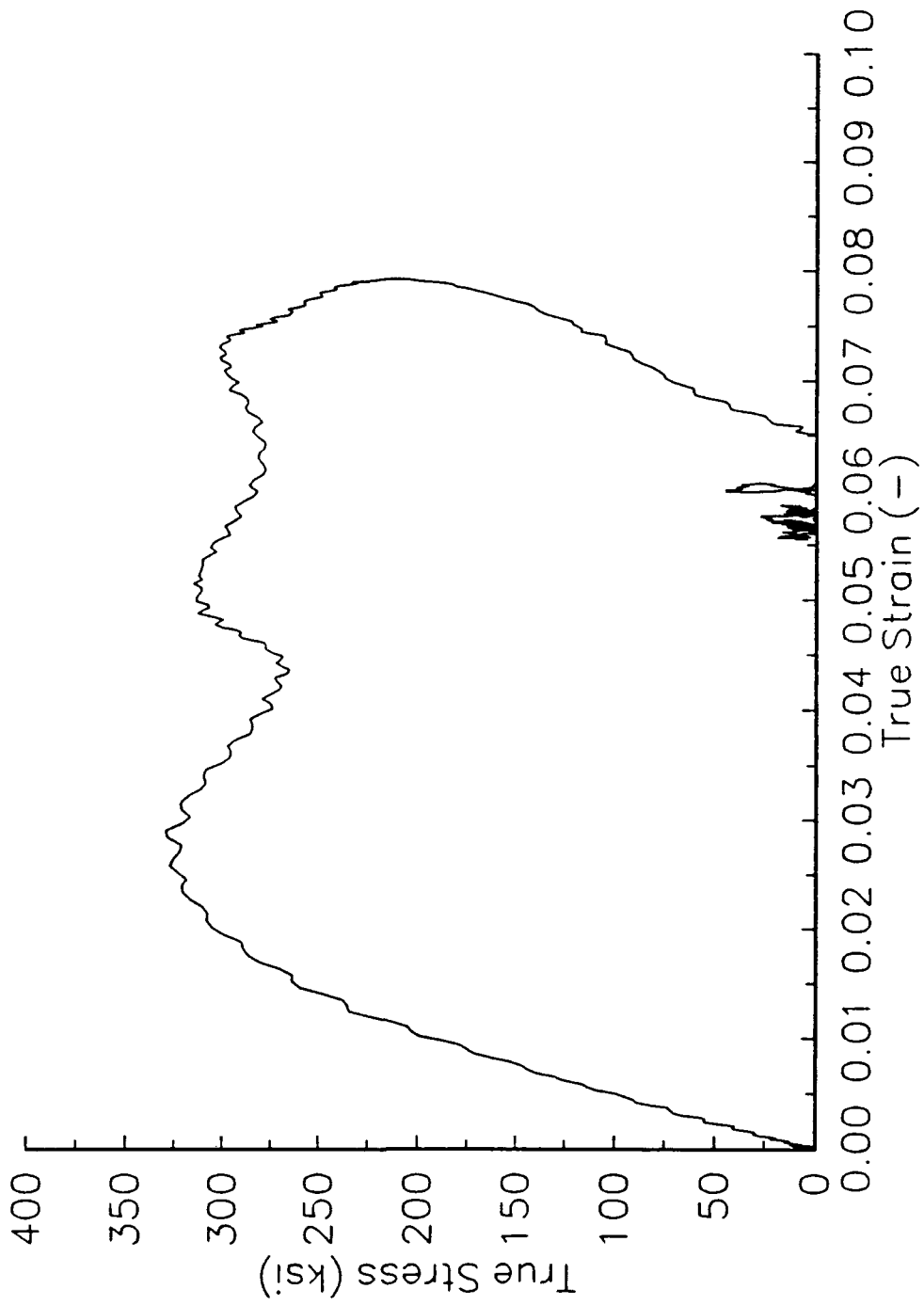


FIG. 2(a)

W2HF2  
L = 0.1275", D = 0.2502"; Strain rate = 2500/s

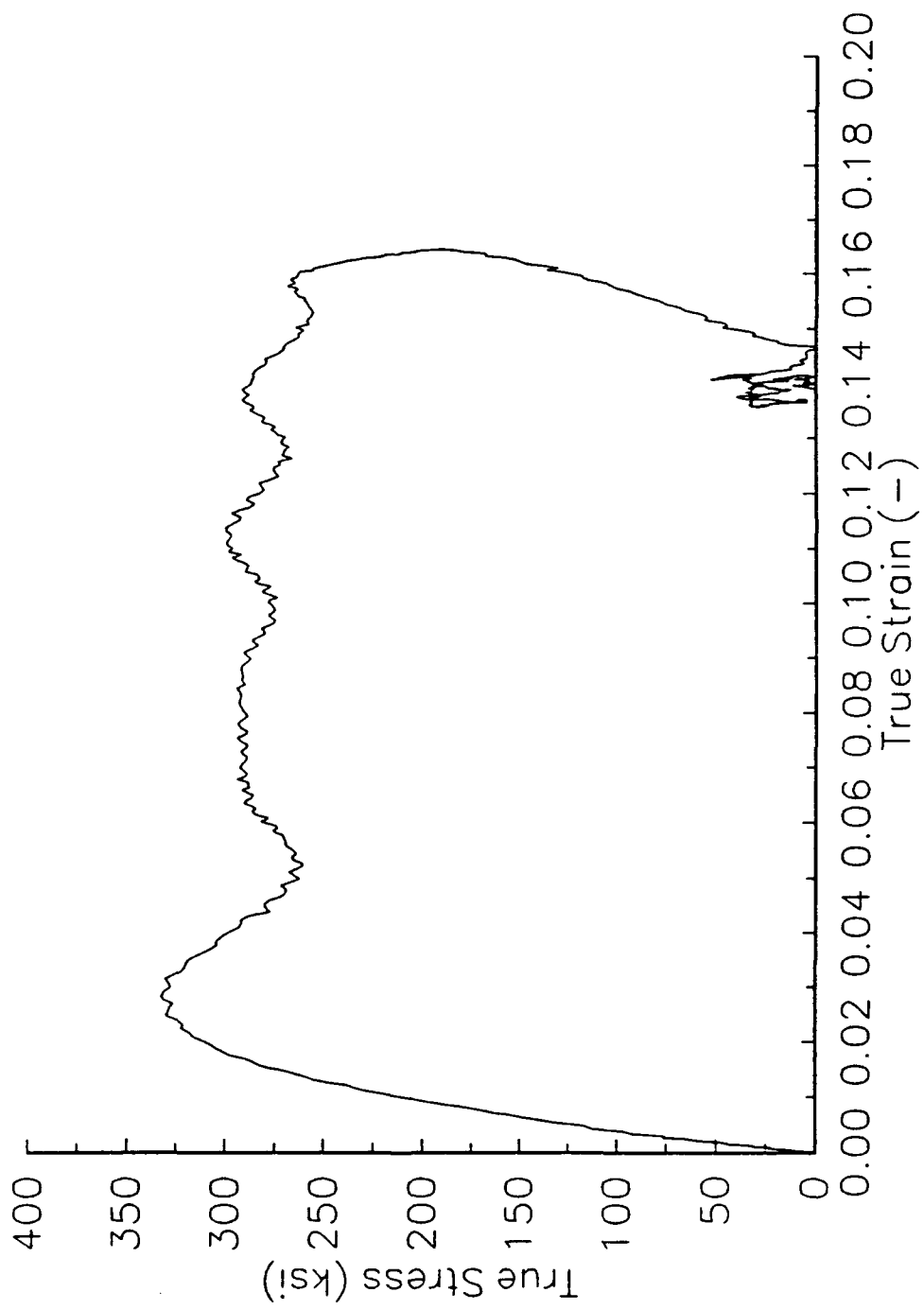


FIG. 2(b)

W-2Hf-3-LOAD1  
L = 0.1282", D = 0.25"; Strain Rate = 350/s

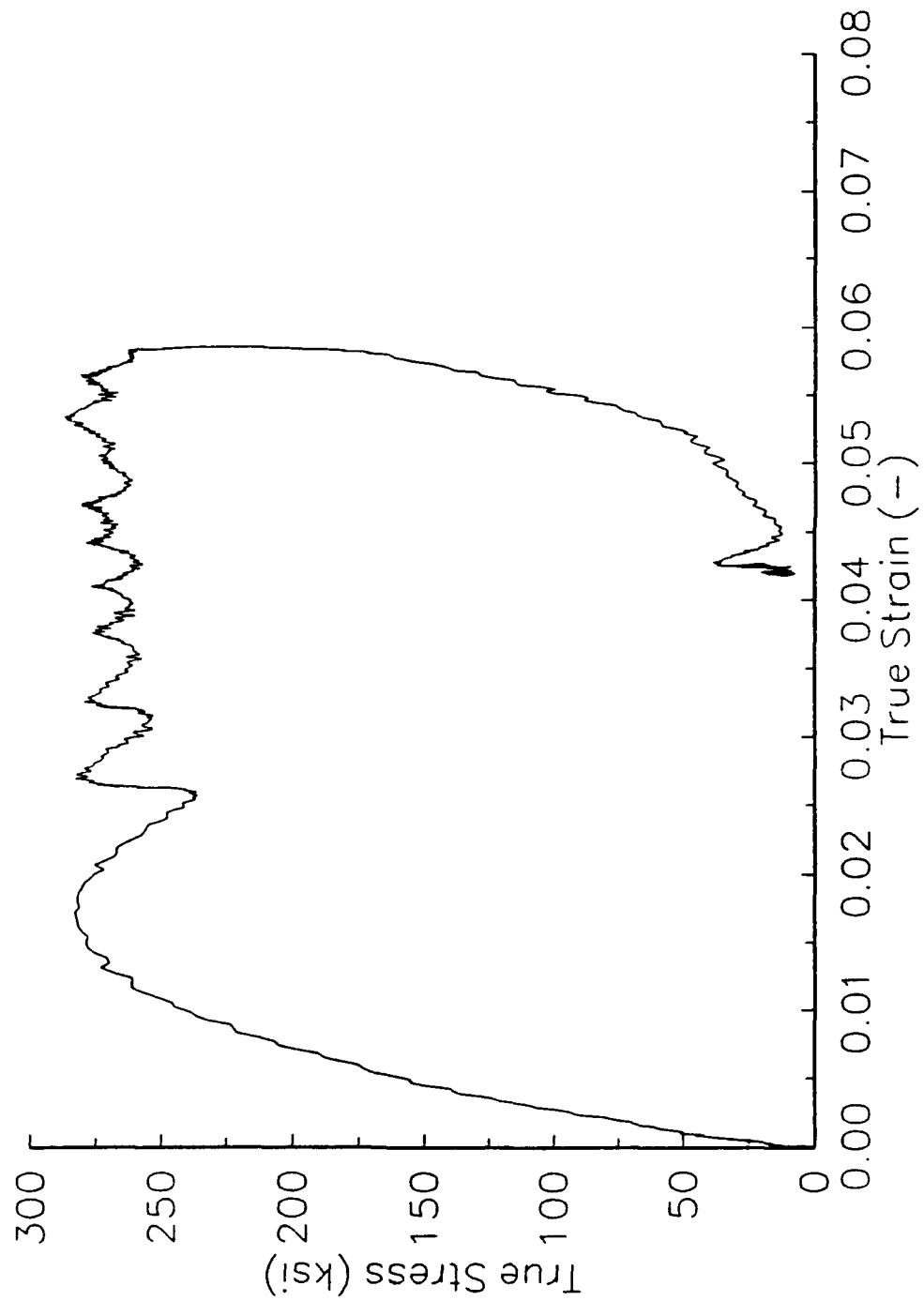


FIG. 2(C)

W-2Hf-3-LOAD2  
L = 0.1156", D = 0.2641"; Strain Rate = 650/s

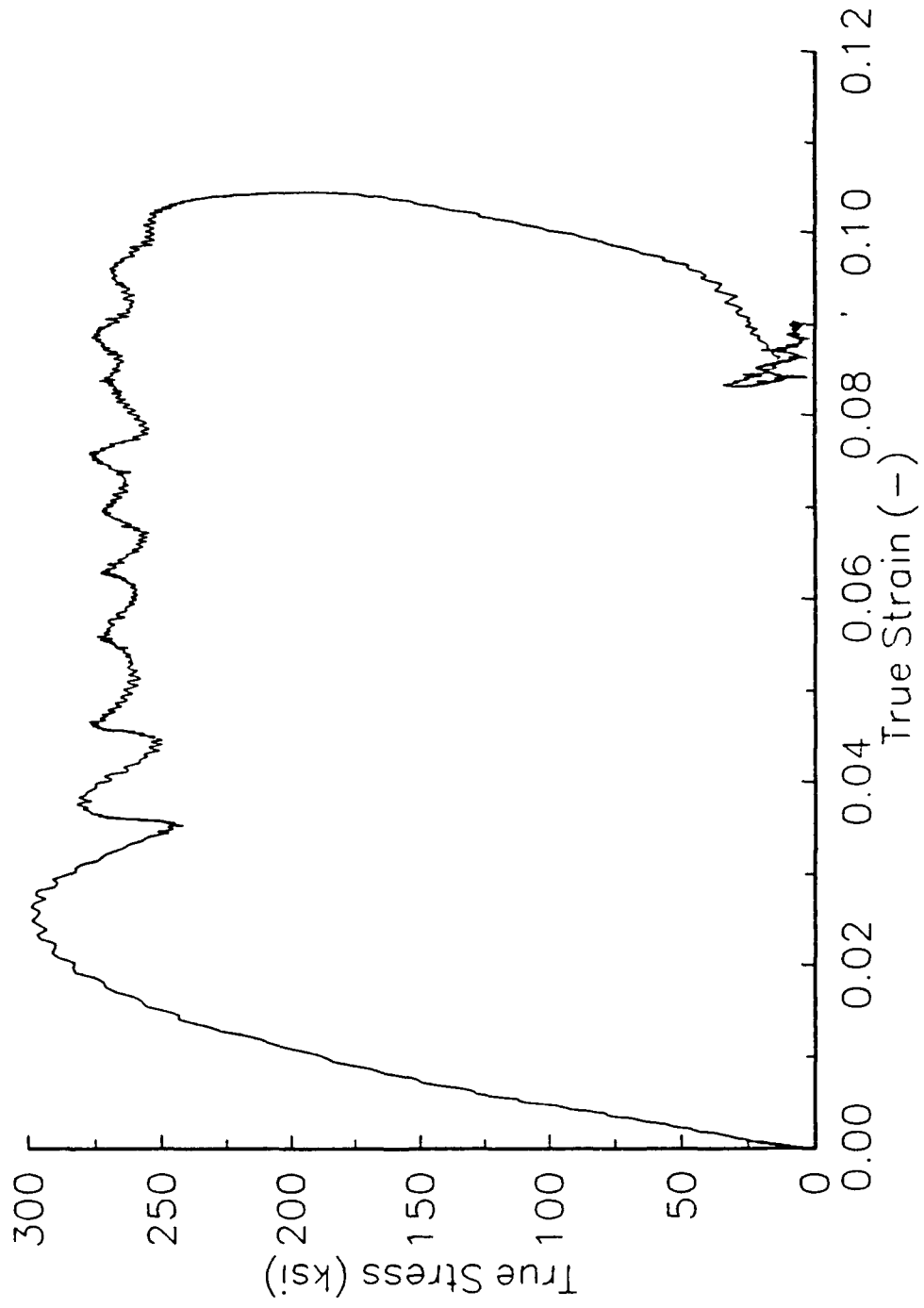


FIG. 2(d)

W-2Hf-4  
L = 0.1283", D = 0.2495", ; Strain Rate = 2000/s

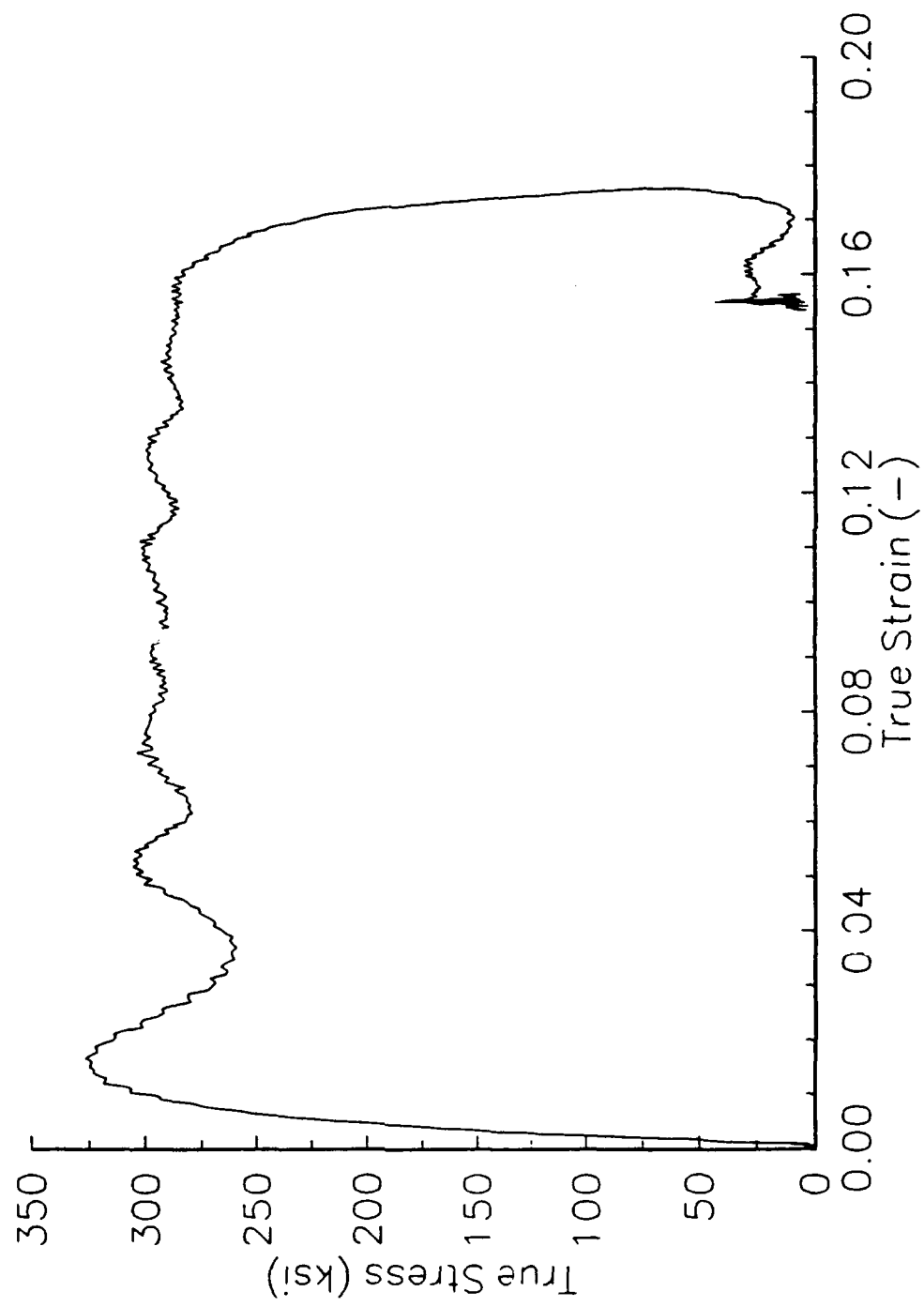


FIG. 2(e)

W-2Hf-5  
L = 0.1277", D = 0.2498"; Strain Rate = 3600/s

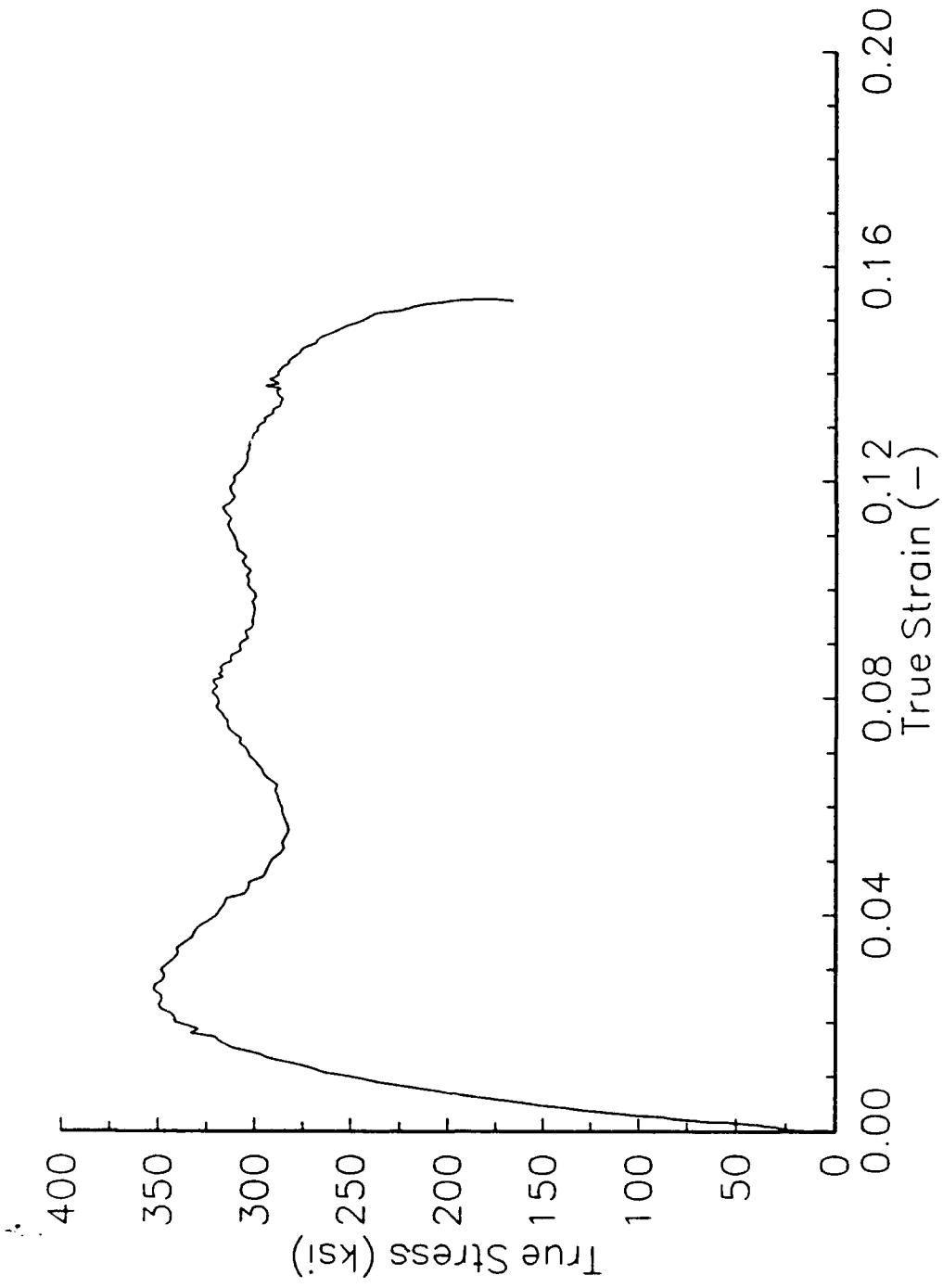


FIG. 2(f)

W1 OHF1  
L = .1267", D = 0.25" ; Strain Rate = 1700/s

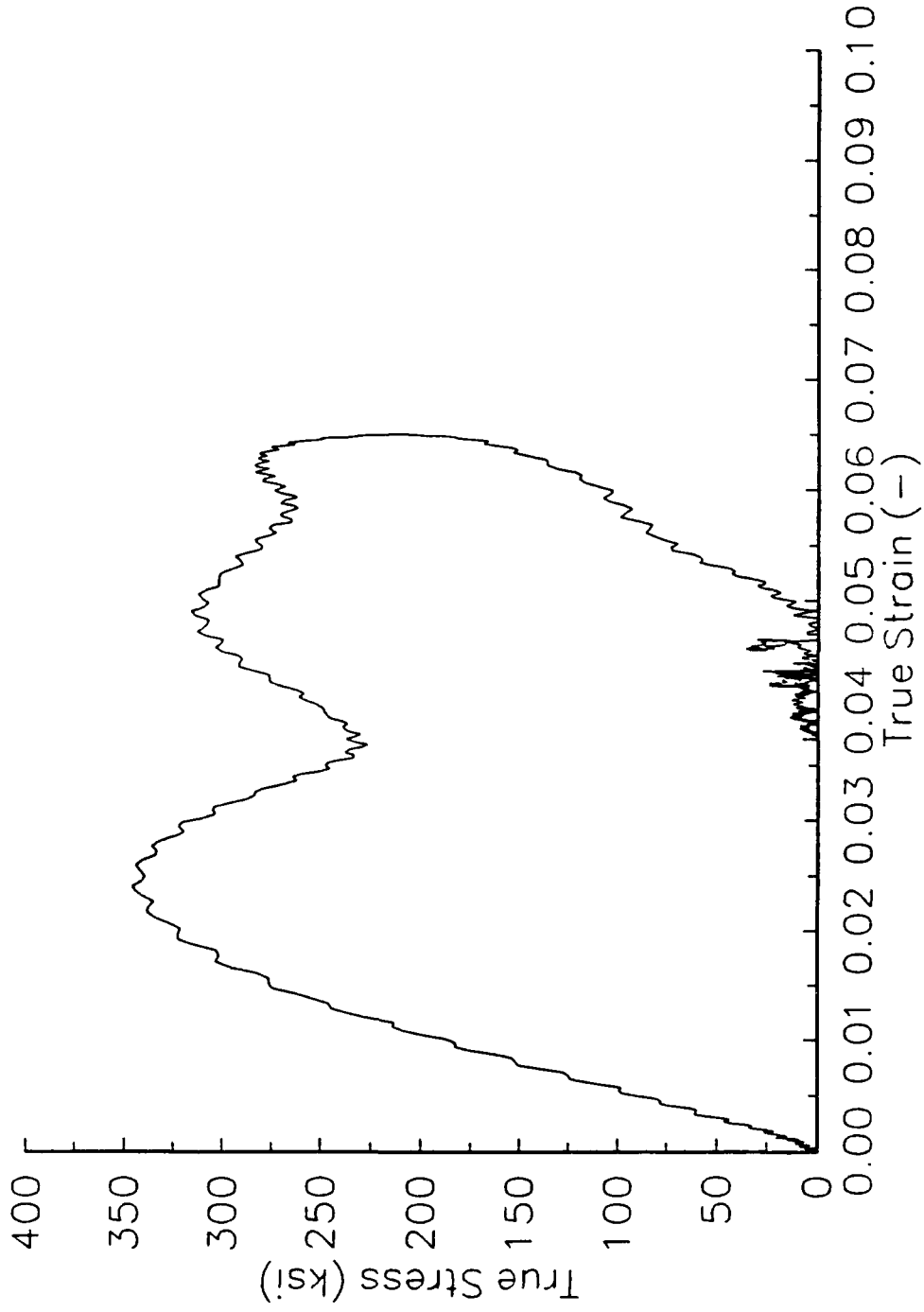


FIG. 3(a)



W1 OHF2

L = 0.1267", D = 0.2499" ; Strain Rate = 2200/s

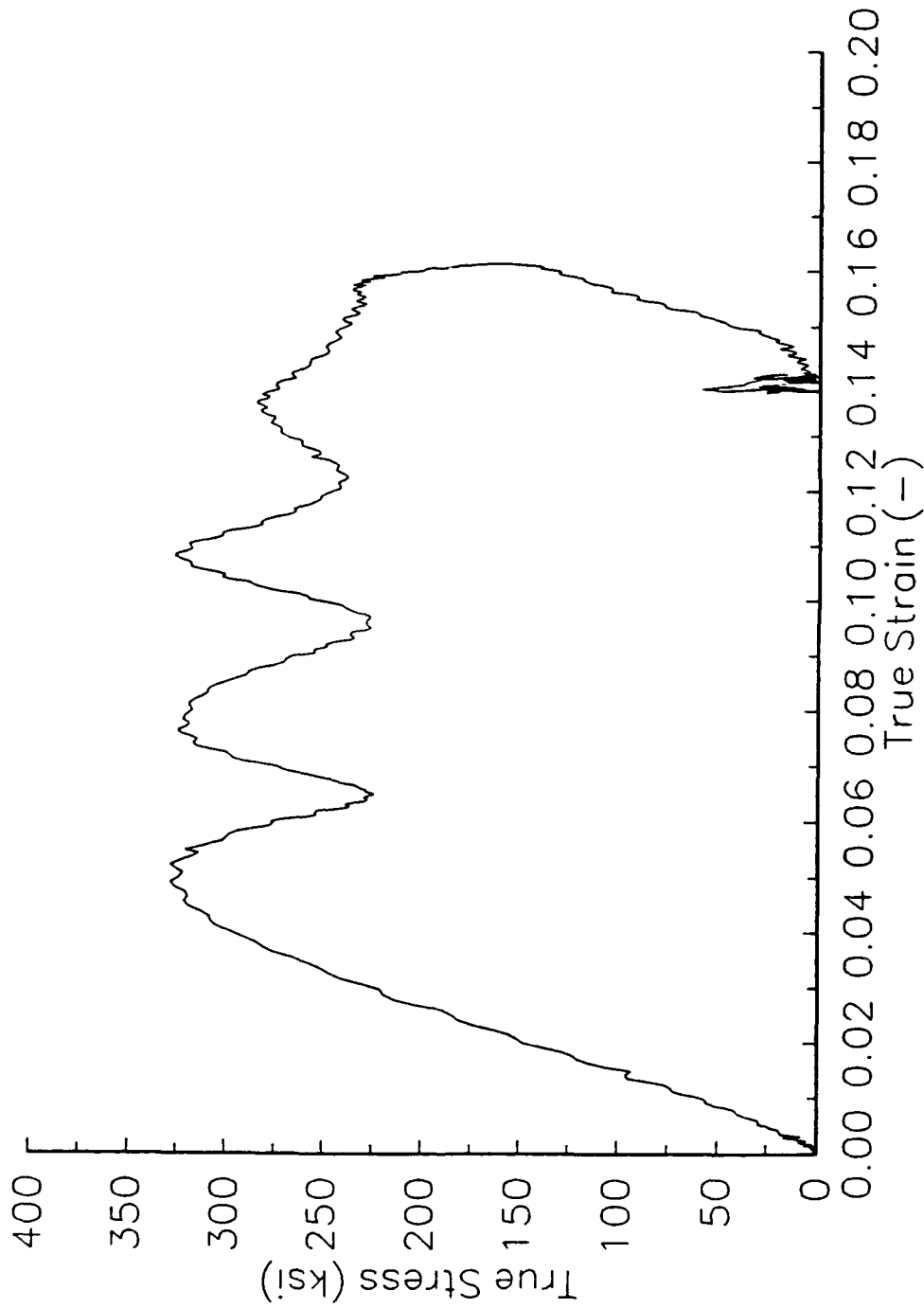


FIG. 3(b)

W-1 OHf-3  
L = 0.1266", L = 0.2503" ; Strain Rate = 750/s

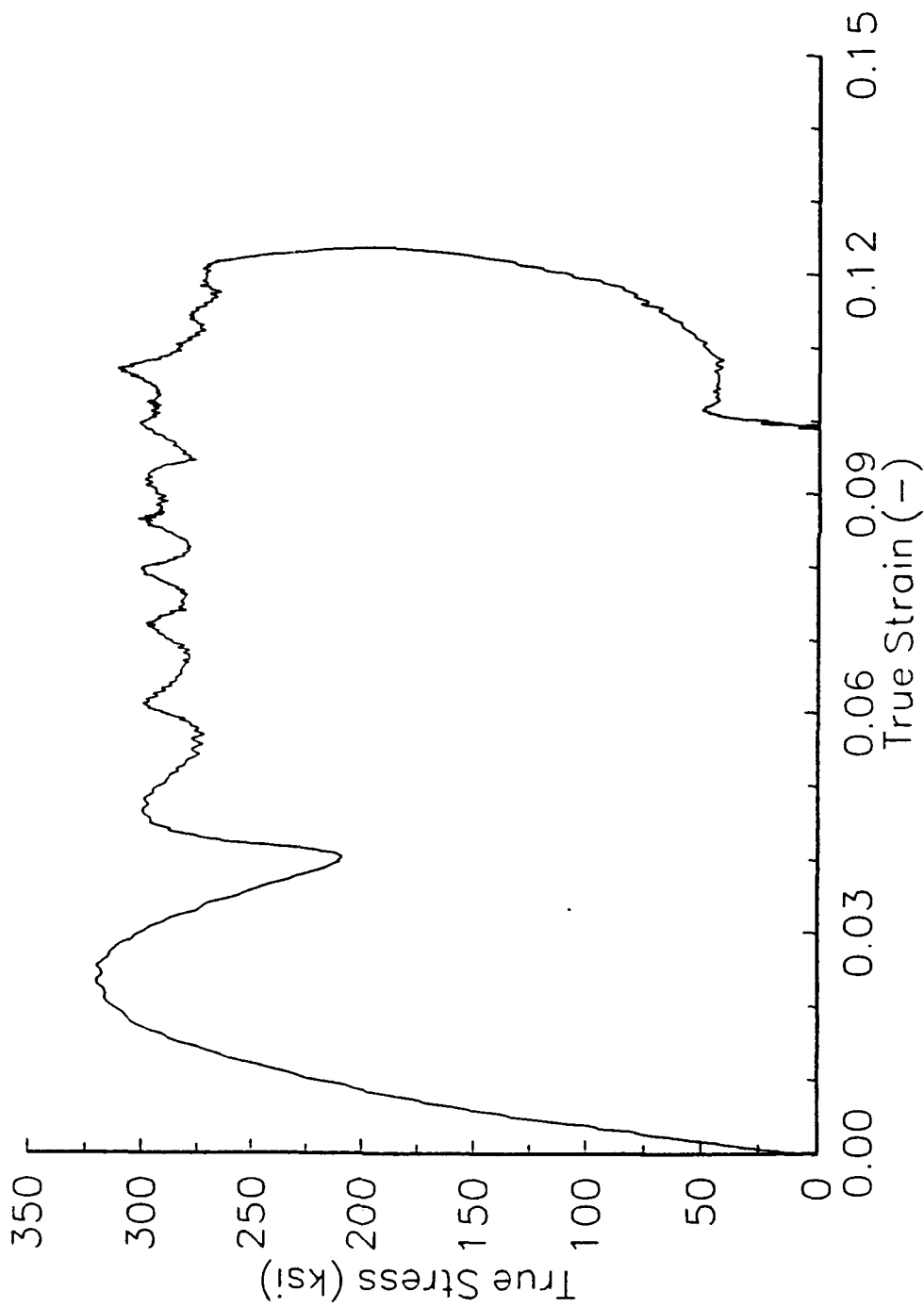


FIG. 3(C)

W-10Hf-4  
L = 0.1268", D = 0.2503" ; Strain Rate = 2000/s

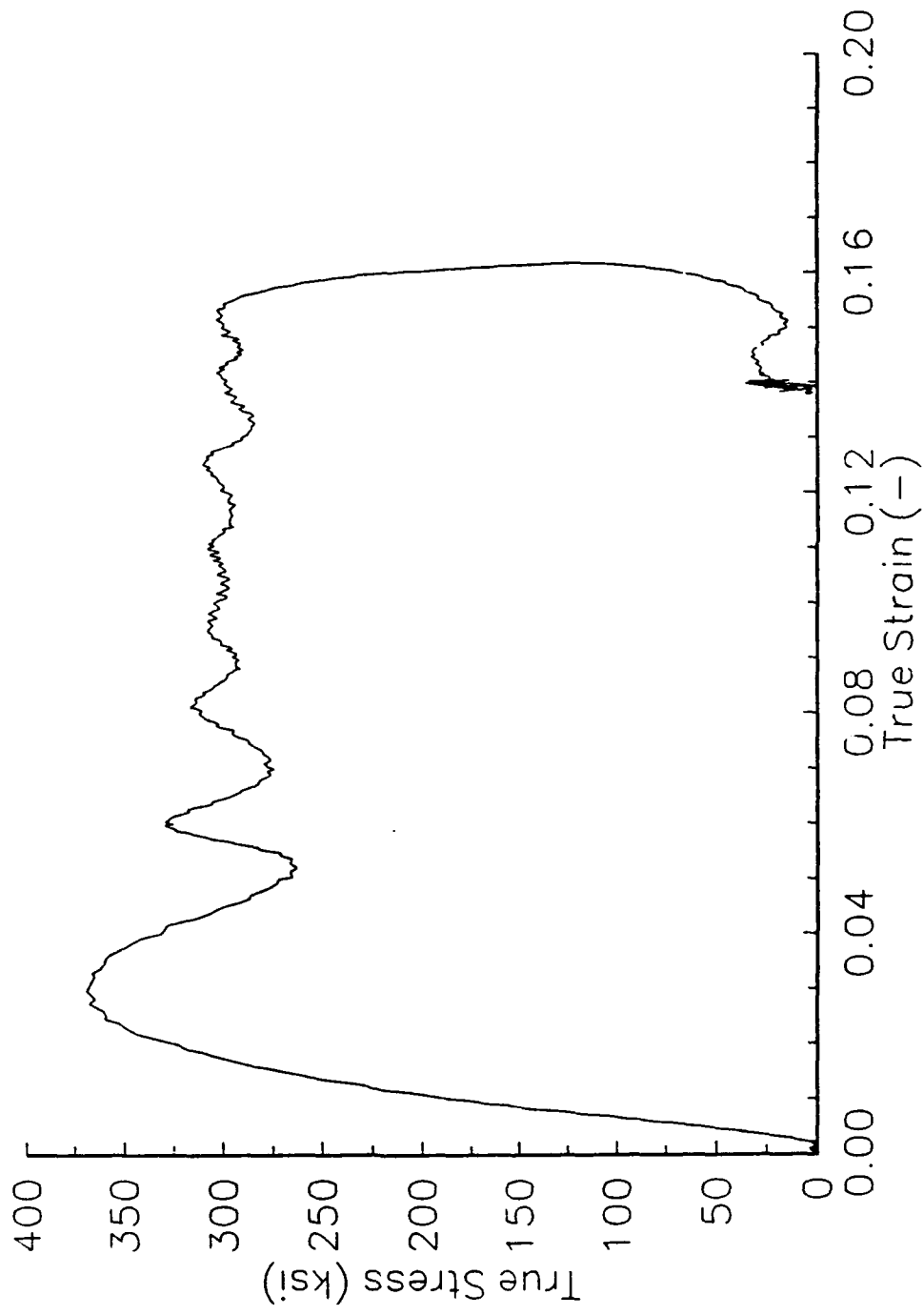


FIG. 3(d)

W-10Hf-5  
L = 0.128", D = 0.2498"; Strain Rate = 3000/s

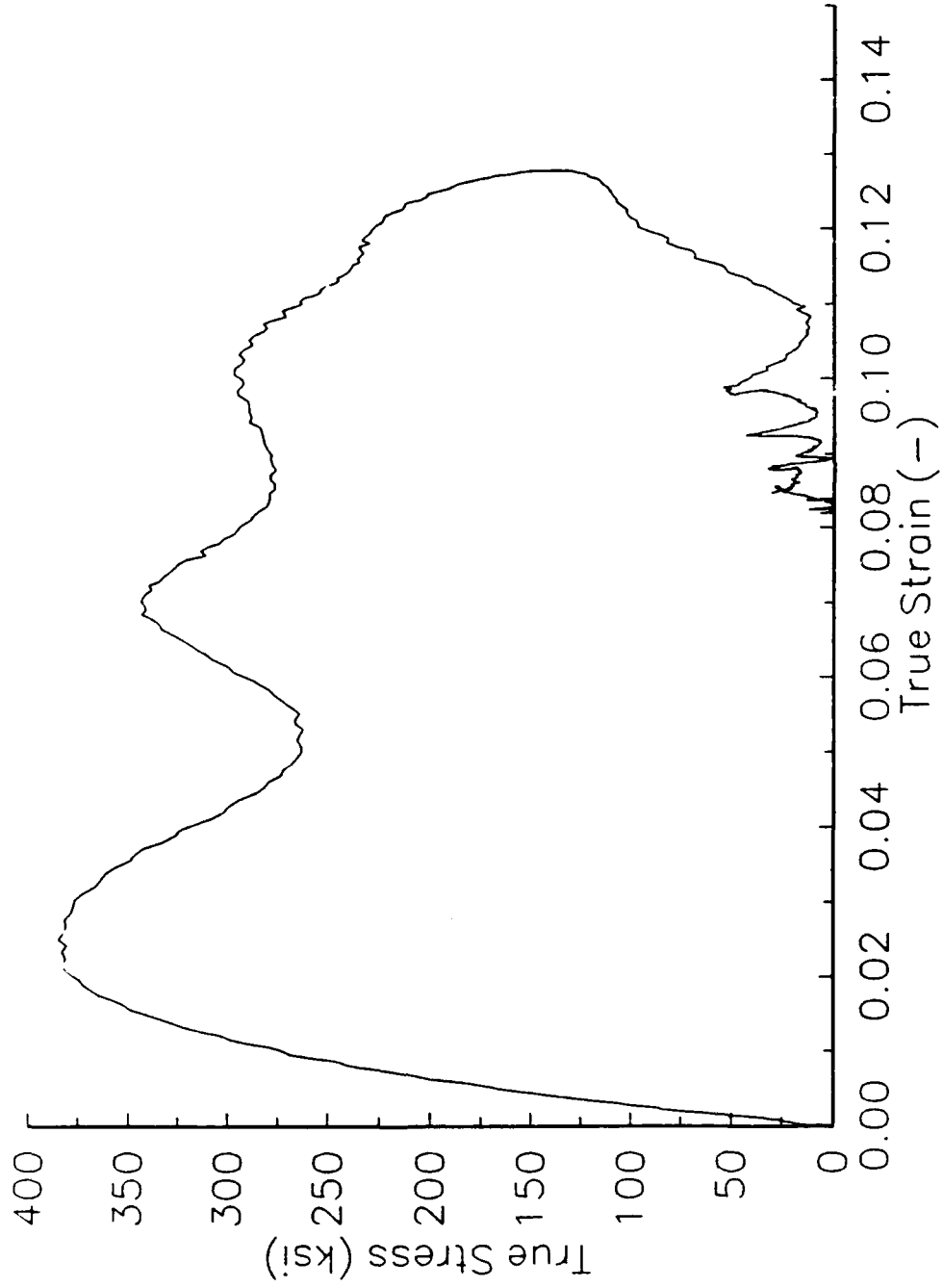
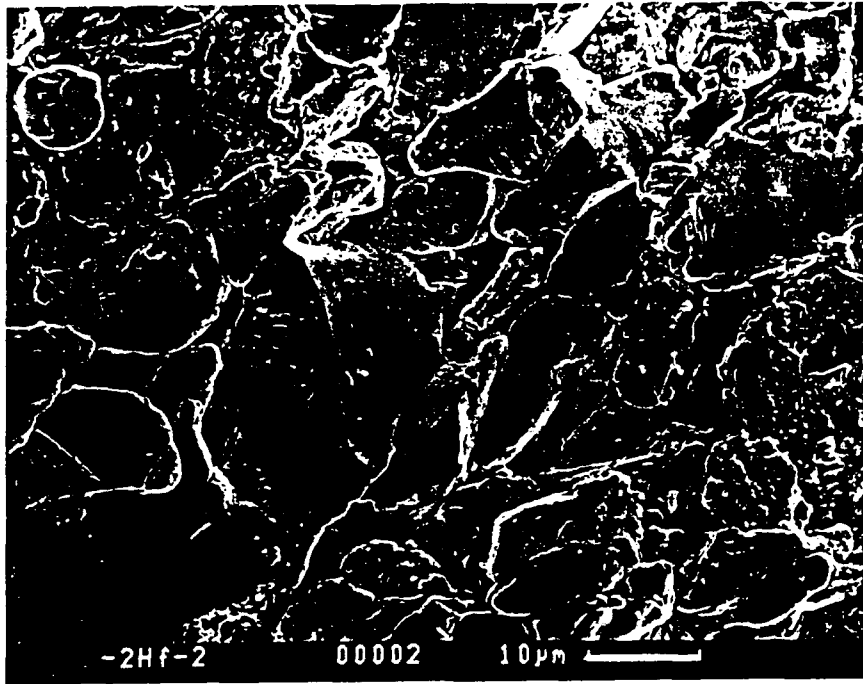
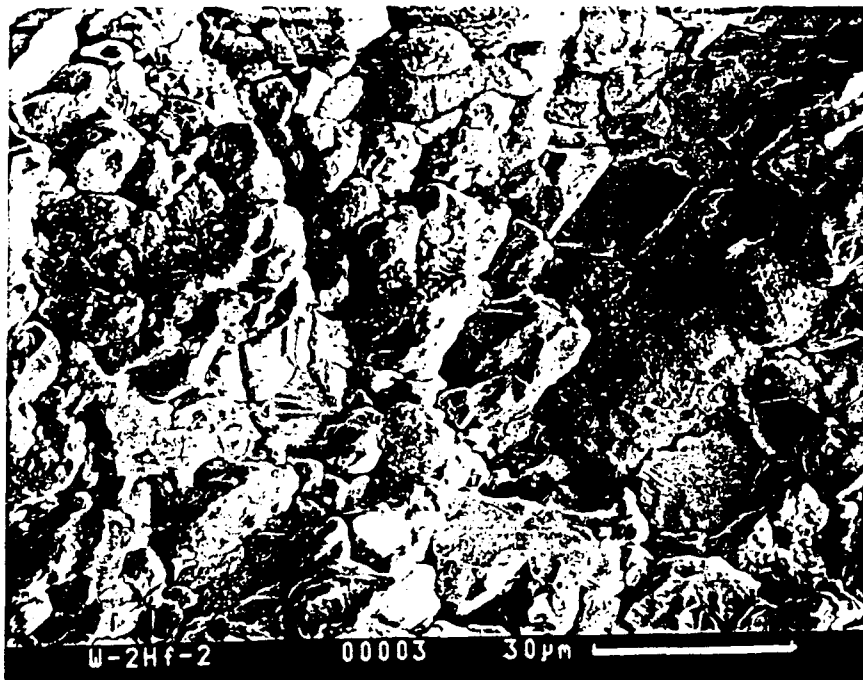


FIG. 3(e)

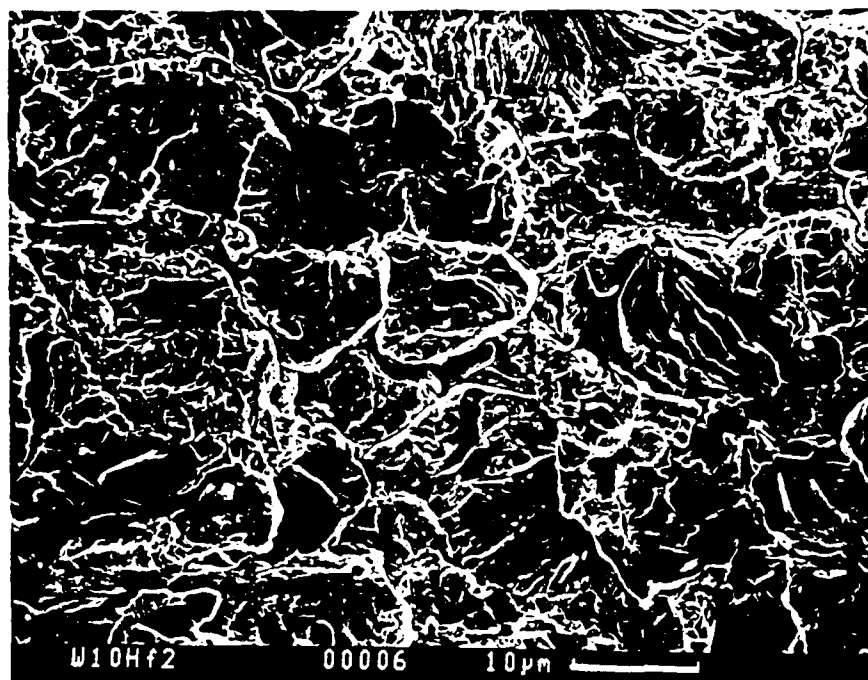


(a)

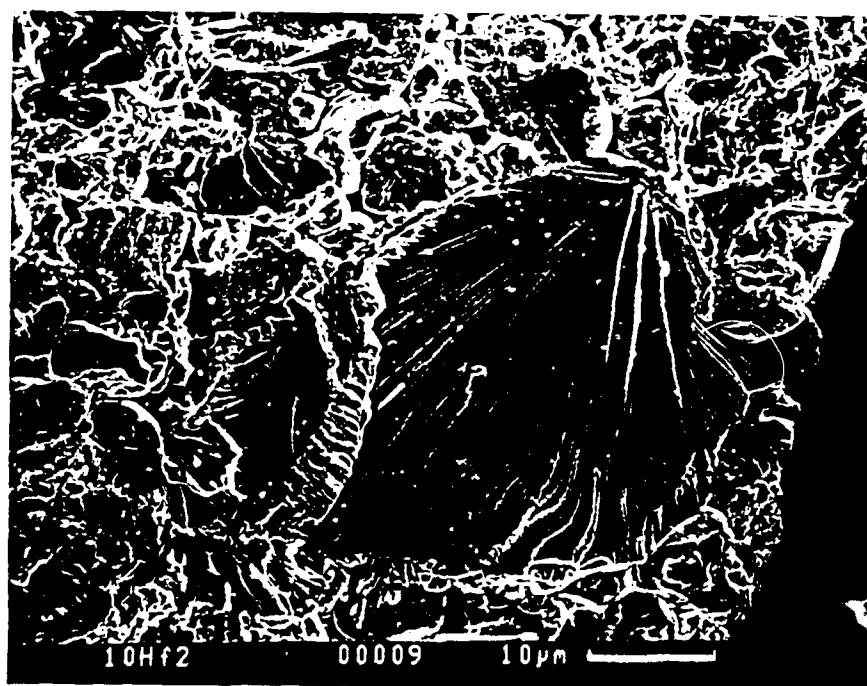


(b)

FIG. 4



(a)



(b)

FIG. 5

Dear Brian:

These are some results and ideas on Hafnium using the Split Hopkinson Pressure Bar

Fig: 1 - a geometry known as the Localize top hat specimen used for strain localization studies.

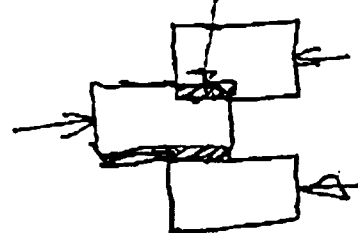
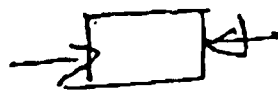


Fig: 2 - Results from a Hf top hat specimen. Observe the gradual drop in load - indicating localization.

Fig: 3 : High strain rate behavior of Hf @  $\dot{\epsilon} = 10^3$  and  $1.5 \times 10^3/s$ . Cylindrical samples were used



Ask Jack if you have questions!  
He knows about these results.

FIG: 2

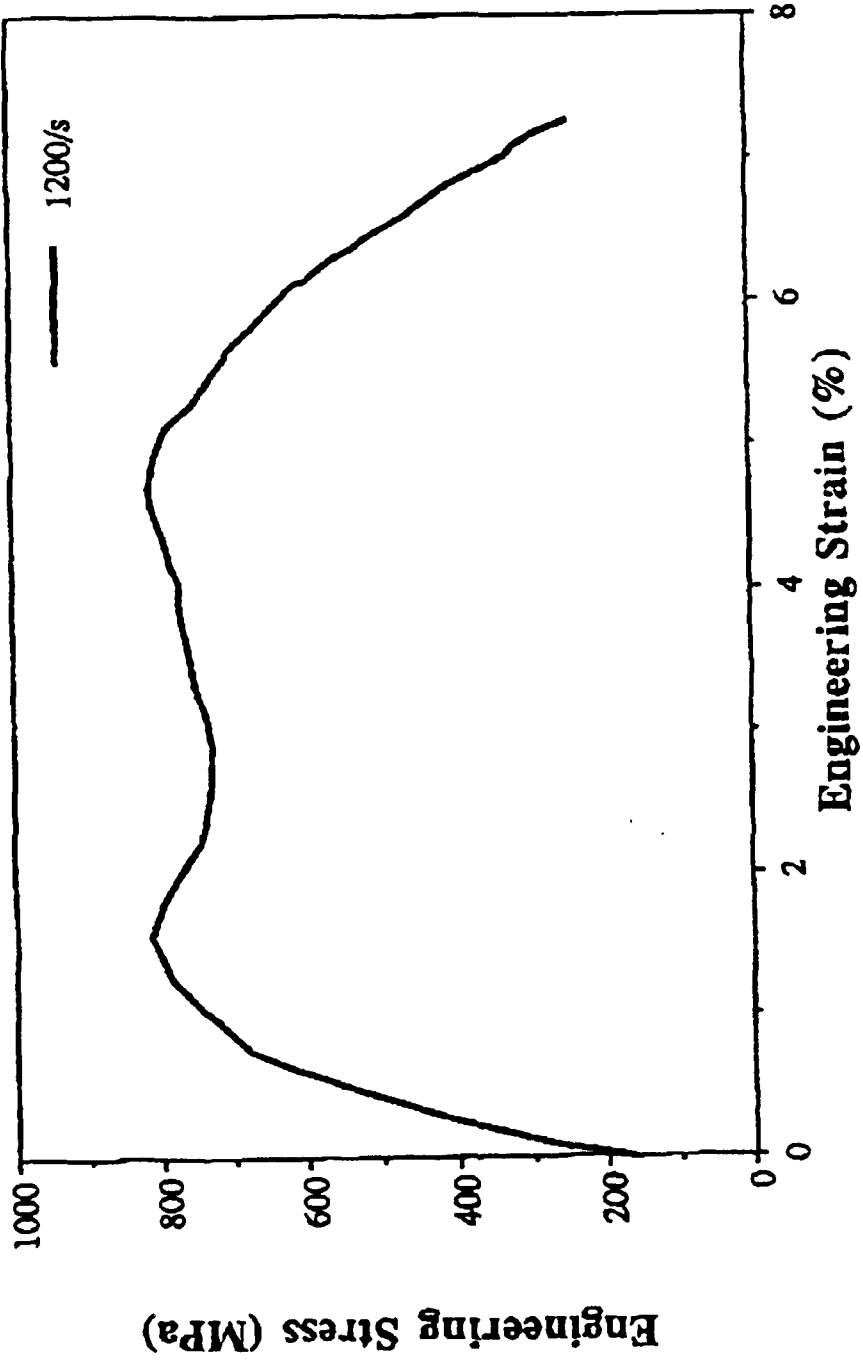
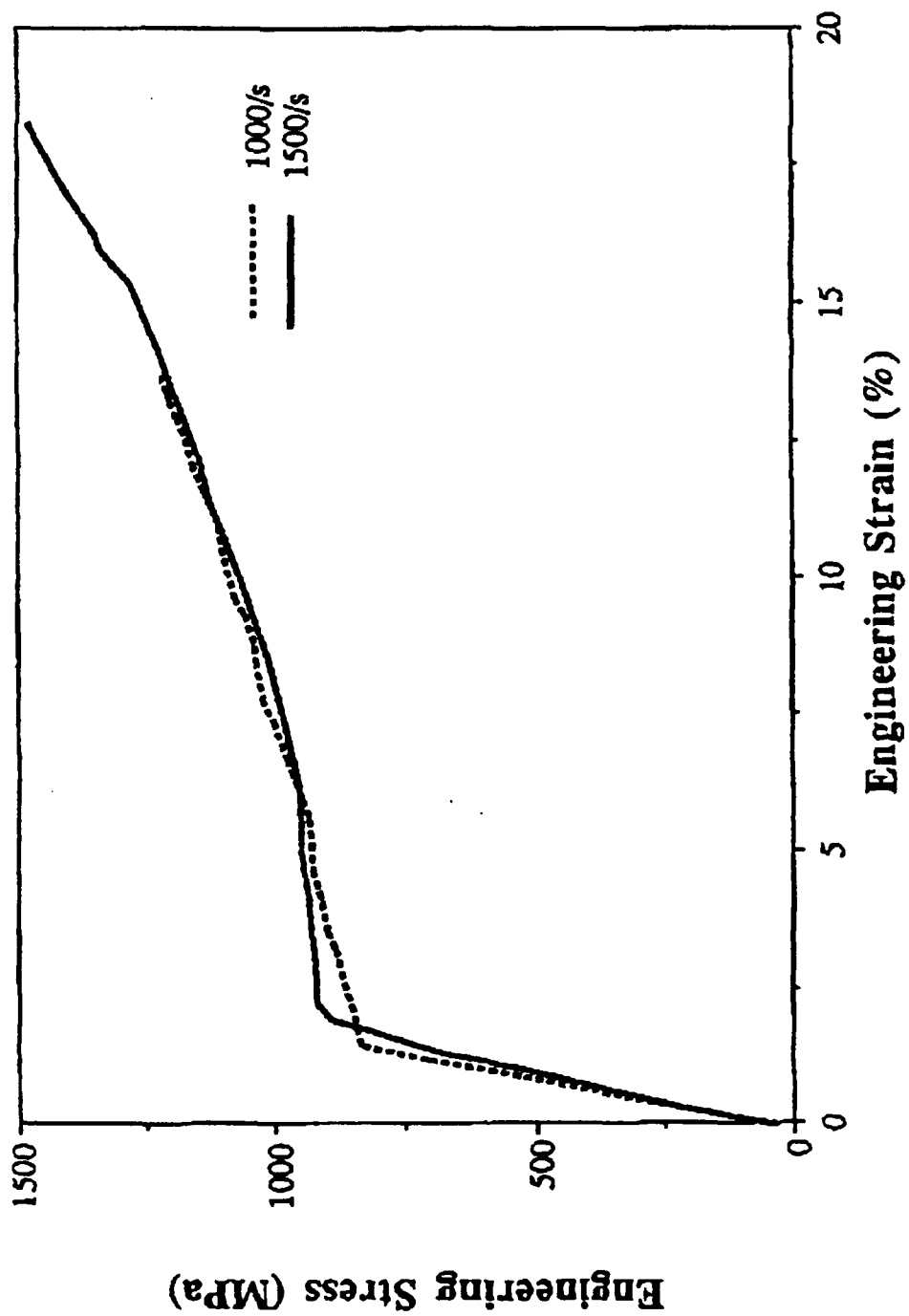




FIG:3



*HF solid cyl.*

---

**Distribution List**

---

1 Office of the Secretary of Defense for Research and Engineering, The Pentagon, Washington, D.C. 20301

Commander, U.S. Army Laboratory Command, 2800 Powder Mill Road, Adelphi, MD 20783-1145

1 ATTN: AMSLC-IM-TL

1 ATTN: AMSLC-CT

Commander, Defense Technical Information Center, Cameron Station, Building 5, 5010 Duke Street, Alexandria, VA 22304-6145

2 DTIC-FDAC

1 MIAC/CINDAS, Purdue University, 2595 Yeager Road, West Lafayette, IN 47905

Commander, Army Research Office, P.O. Box 12211, Research Triangle Park, NC

27709-2211

1 ATTN: Information Processing Office

1 Dr. Andrew Crowson

Dr. Edward Chen

Commander U.S. Army Materiel Command (AMC), 5001 Eisenhower Avenue, Alexandria, VA 22333

1 ATTN: AMCSCI

Commander, U.S. Army Materiel Systems Analysis Activity, Aberdeen Proving Ground, MD 21005

1 ATTN: AMXSU-MP, Director

Commander, U.S. Army Missile Command, Redstone Scientific Information Center, Redstone Arsenal, AL 35898-5241

1 ATTN: AMSMI-RD-CS-R/Doc

Commander, U.S. Army Armament Research Development and Engineering Center, Dover, NJ 07801

1 ATTN: Technical Library

1 Mr. D. Kapoor

1 Dr. S. Cytron

Commander, U.S. Army Tank-Automotive Command, Warren, MI 48397-5000

2 ATTN: AMSTA-TSL Technical Library

Commander, U.S. Army Foreign Science and Technology Center, 220 7th Street, N.E., Charlottesville, VA 22901

3 ATTN: AIFRTC, Applied Technologies Branch, Gerald Schlesinger

Naval Research Laboratory, Washington, D.C. 20375

1 ATTN: Code 5830

1 Code 2627

Chief of Naval Research, Arlington, VA 22217

1 ATTN: Code 471

Naval Surface Weapons Center, Dahlgren Laboratory, Dahlgren, VA  
22448

1 ATTN: Code G-32, Ammunition Branch, Mr. Brian Sabourin

Commander, Rock Island Arsenal, Rock Island, IL 61299-6000

1 ATTN: SMCRI-SEM-T

Battelle Columbus Laboratories, Battelle Memorial Institute, 505  
King Avenue, Columbus, OH 43201

1 ATTN: Mr. Henry Cialone

1 Dr. Alan Clauer

Battelle Pacific Northwest Laboratories, P.O. Box 999, Richland,  
WA 99352

1 ATTN: Mr. William Gurwell

1 Dr. Gordon Dudder

GTE Sylvania, Inc. Chemical and Metallurgical Division, Hawes  
Street, Towanda, PA 18848

1 ATTN: Dr. James Mullendore

1 Mr. James Spencer

Director, Ballistic Research Laboratory, Aberdeen Proving Ground,  
MD 21005

1 ATTN: SLCBR-TSB-S (STINFO)

1 SLCBR-TB-P, Mr. Lee Magness

Teledyne Firth Sterling, 1 Teledyne Place, LaVergne, TN 37086

1 ATTN: Dr. Steven Caldwell

1 Dr. Thomas Penrice

Technology Associates Corp., 17911 Sampson Lane, Huntington  
Beach, CA

92647

1 ATTN: Dr. Gary Allen

Los Alamos National Laboratory, ATAC, MS F681, P.O. Box 1663, Los  
Alamos, NM 87545

1 ATTN: Dr. Bill Hogan

Philips Elmet, 1560 Lisbon Road, Lewiston, ME 04240

1 ATTN: Mr. James Anderson

Ultramet, Inc., 12173 Montague Street, Pacoima, CA 91331

1 ATTN: Dr. J.J. Stiglich

1 Mr. Brian Williams

1 Dr. Robert Tuffias

Ceracon, Inc., 1101 N. Market Boulevard, Suite 9, Sacramento, CA  
95834

1 ATTN: Dr. Ramas Raman

Southwest Research Institute, 6220 Culebra Road, P.O. Drawer  
28510, San Antonio, TX 78228-0510

1 ATTN: Dr. Animesh Bose

1 Dr. James Lankford

Metalworking Technology, Inc., 1450 Scalp Avenue, Johnstown, PA  
15904

1 ATTN: Mr. C. Buck Skena

1 Mr. Timothy McCabe

Research Triangle Institute, P.O. Box 12194, Research Triangle  
Park, NC 27709-2154

1 ATTN: Dr. John B. Posthill

3C Systems, 620 Arglye Road, Wynnewood, PA 19096

1 ATTN: Mr. Murray Kornhauser

Advance Technology Coatings, 300 Blue Smoke Ct. West, Fort Worth,  
TX 76105

1 ATTN: Mr. Grady Sheek

Alliant Techsystems, 7225 Northland Drive, Brooklyn Park, MN  
55428

1 ATTN: Dr. Stan Nelson

1 Mr. Mark Jones

1 Mr. Thomas Steigauf

CAMDEC, 3002 Dow Avenue, Suite 110, Tustin, CA 92680

1 ATTN: Dr. Richard Harlow

Chamberlain Manufacturing Co., 550 Esther St., P.O. Box 2545,  
Waterloo, IA

50704

1 ATTN: Mr. Tom Lynch

Defense Technology International, Inc., The Stark House, 22  
Concord Street,

Nashua, NH

1 ATTN: Mr. Douglas Ayer

Materials and Electrochemical Research Corporation, 7960 S. Kolb  
Road, Tucson, AZ 85706

1 ATTN: Dr. James Withers

1 Dr. Sumit Guha

Materials Modification, Inc., 2929-P1 Eskridge Center, Fairfax,  
VA 22031

1 ATTN: Dr. T.S. Sudarshan

Micro Materials Technology, 120-D Research Drive, Milford, CT  
06460

1 ATTN: Dr. Richard Cheney

Nuclear Metals, 2229 Main Street, Concord, MA 01742

1 ATTN: Dr. Willian Nachtrab

Olin Ordnance, 10101 9th Street N., St. Petersburg, FL

1 ATTN: Hugh McElroy

The Pennsylvania State University, Department of Engineering  
Science and Mechanics, 227 Hammond Building, University Park, PA  
16802-1401

1 ATTN: Dr. Randall M. German, Professor, Brush Chair in  
Materials

Director, U.S. Army Materials Technology Laboratory, Watertown,  
MA 02172-0001

2 ATTN: SLCMT-TML

1 SLCMT-IMA-V

1 SLCMT-PRC

20 SLCMT-MEM, Mr. Robert Dowding

U.S. Army Materials Technology Laboratory  
Watertown, Massachusetts 02172-0001  
HAFFIUM-TITANIUM-COATED TUNGSTEN POWDERS FOR  
KINETIC ENERGY PENETRATORS, PHASE I, SBIR  
Brian E. Williams and Jacob J. Stiglich, Jr.  
Ultramet, Pacoima, CA 91331

AD

UNCLASSIFIED  
UNLIMITED DISTRIBUTION

Key Words

Tungsten powders  
Composites  
Chemical vapor  
deposition (CVD)

Technical Report MTL TR 92-36, May 1992, 71 pp -  
illus-tables, Contract DAAL04-91-C-5022  
Final Report, Feb 91 - Oct 91

Depleted uranium (DU) is the state-of-the-art material for kinetic energy penetrators used to defeat steel and composite armors. DU alloys, however, are costly to fabricate, handle, and store because of their extremely complex metallurgy and the obvious health considerations associated with the use of uranium. Tungsten composite materials are also used in kinetic energy penetrators, offering easier and safer fabrication, handling, and storage but to date lacking the performance of DU. The mechanisms by which a penetrator defeats an armor are difficult to determine, either experimentally or from first principles. Recent experiments have identified the presence of an "adiabatic shear" mechanism that appears to be important in the penetration of rolled homogeneous armor (RHA) by DU penetrators. In this program, Ultramet proposed to apply hafnium and titanium coatings to tungsten powder (W<sub>p</sub>) particles by chemical vapor deposition (CVD) using an established fluidized-bed powder coating technique. Both hafnium and titanium are known to exhibit the adiabatic shear phenomenon. High strain rate experiments ( $\approx 10^4$ /sec) were performed on Ti(6Al-4V) and monolithic hafnium materials in order to establish the presence or absence of this mode of deformation in small cylindrical specimens. In addition, specimens of 2 wt% CVD Hf/W<sub>p</sub> and 2 wt% CVD Hf + 8 wt% powder-mixed Hf/W<sub>p</sub> were tested at high strain rate conditions ( $\approx 10^4$ /sec).

U.S. Army Materials Technology Laboratory  
Watertown, Massachusetts 02172-0001  
HAFFIUM-TITANIUM-COATED TUNGSTEN POWDERS FOR  
KINETIC ENERGY PENETRATORS, PHASE I, SBIR  
Brian E. Williams and Jacob J. Stiglich, Jr.  
Ultramet, Pacoima, CA 91331

AD

UNCLASSIFIED  
UNLIMITED DISTRIBUTION

Key Words

Tungsten powders  
Composites  
Chemical vapor  
deposition (CVD)

Technical Report MTL TR 92-36, May 1992, 71 pp -  
illus-tables, Contract DAAL04-91-C-5022  
Final Report, Feb 91 - Oct 91

Depleted uranium (DU) is the state-of-the-art material for kinetic energy penetrators used to defeat steel and composite armors. DU alloys, however, are costly to fabricate, handle, and store because of their extremely complex metallurgy and the obvious health considerations associated with the use of uranium. Tungsten composite materials are also used in kinetic energy penetrators, offering easier and safer fabrication, handling, and storage but to date lacking the performance of DU. The mechanisms by which a penetrator defeats an armor are difficult to determine, either experimentally or from first principles. Recent experiments have identified the presence of an "adiabatic shear" mechanism that appears to be important in the penetration of rolled homogeneous armor (RHA) by DU penetrators. In this program, Ultramet proposed to apply hafnium and titanium coatings to tungsten powder (W<sub>p</sub>) particles by chemical vapor deposition (CVD) using an established fluidized-bed powder coating technique. Both hafnium and titanium are known to exhibit the adiabatic shear phenomenon. High strain rate experiments ( $\approx 10^4$ /sec) were performed on Ti(6Al-4V) and monolithic hafnium materials in order to establish the presence or absence of this mode of deformation in small cylindrical specimens. In addition, specimens of 2 wt% CVD Hf/W<sub>p</sub> and 2 wt% CVD Hf + 8 wt% powder-mixed Hf/W<sub>p</sub> were tested at high strain rate conditions ( $\approx 10^4$ /sec).

U.S. Army Materials Technology Laboratory  
Watertown, Massachusetts 02172-0001  
HAFFIUM-TITANIUM-COATED TUNGSTEN POWDERS FOR  
KINETIC ENERGY PENETRATORS, PHASE I, SBIR  
Brian E. Williams and Jacob J. Stiglich, Jr.  
Ultramet, Pacoima, CA 91331

AD

UNCLASSIFIED  
UNLIMITED DISTRIBUTION

Key Words

Tungsten powders  
Composites  
Chemical vapor  
deposition (CVD)

Technical Report MTL TR 92-36, May 1992, 71 pp -  
illus-tables, Contract DAAL04-91-C-5022  
Final Report, Feb 91 - Oct 91

Depleted uranium (DU) is the state-of-the-art material for kinetic energy penetrators used to defeat steel and composite armors. DU alloys, however, are costly to fabricate, handle, and store because of their extremely complex metallurgy and the obvious health considerations associated with the use of uranium. Tungsten composite materials are also used in kinetic energy penetrators, offering easier and safer fabrication, handling, and storage but to date lacking the performance of DU. The mechanisms by which a penetrator defeats an armor are difficult to determine, either experimentally or from first principles. Recent experiments have identified the presence of an "adiabatic shear" mechanism that appears to be important in the penetration of rolled homogeneous armor (RHA) by DU penetrators. In this program, Ultramet proposed to apply hafnium and titanium coatings to tungsten powder (W<sub>p</sub>) particles by chemical vapor deposition (CVD) using an established fluidized-bed powder coating technique. Both hafnium and titanium are known to exhibit the adiabatic shear phenomenon. High strain rate experiments ( $\approx 10^4$ /sec) were performed on Ti(6Al-4V) and monolithic hafnium materials in order to establish the presence or absence of this mode of deformation in small cylindrical specimens. In addition, specimens of 2 wt% CVD Hf/W<sub>p</sub> and 2 wt% CVD Hf + 3 wt% powder-mixed Hf/W<sub>p</sub> were tested at high strain rate conditions ( $\approx 10^4$ /sec).

U.S. Army Materials Technology Laboratory  
Watertown, Massachusetts 02172-0001  
HAFFIUM-TITANIUM-COATED TUNGSTEN POWDERS FOR  
KINETIC ENERGY PENETRATORS, PHASE I, SBIR  
Brian E. Williams and Jacob J. Stiglich, Jr.  
Ultramet, Pacoima, CA 91331

AD

UNCLASSIFIED  
UNLIMITED DISTRIBUTION

Key Words

Tungsten powders  
Composites  
Chemical vapor  
deposition (CVD)

Technical Report MTL TR 92-36, May 1992, 71 pp -  
illus-tables, Contract DAAL04-91-C-5022  
Final Report, Feb 91 - Oct 91

Depleted uranium (DU) is the state-of-the-art material for kinetic energy penetrators used to defeat steel and composite armors. DU alloys, however, are costly to fabricate, handle, and store because of their extremely complex metallurgy and the obvious health considerations associated with the use of uranium. Tungsten composite materials are also used in kinetic energy penetrators, offering easier and safer fabrication, handling, and storage but to date lacking the performance of DU. The mechanisms by which a penetrator defeats an armor are difficult to determine, either experimentally or from first principles. Recent experiments have identified the presence of an "adiabatic shear" mechanism that appears to be important in the penetration of rolled homogeneous armor (RHA) by DU penetrators. In this program, Ultramet proposed to apply hafnium and titanium coatings to tungsten powder (W<sub>p</sub>) particles by chemical vapor deposition (CVD) using an established fluidized-bed powder coating technique. Both hafnium and titanium are known to exhibit the adiabatic shear phenomenon. High strain rate experiments ( $\approx 10^4$ /sec) were performed on Ti(6Al-4V) and monolithic hafnium materials in order to establish the presence or absence of this mode of deformation in small cylindrical specimens. In addition, specimens of 2 wt% CVD Hf/W<sub>p</sub> and 2 wt% CVD Hf + 8 wt% powder-mixed Hf/W<sub>p</sub> were tested at high strain rate conditions ( $\approx 10^4$ /sec).